POLITECNICO DI TORINO

Corso di Laurea Magistrale in Ingegneria Energetica e Nucleare

Comparison between a methanol SAFCell and a traditional SOFC.

Relatore
Marco Masoero
Massimo Santarelli
Correlatore
Marta Gandiglio
Relatore aziendale
Ivano Laganà

Candidato
Salvatore Porretta
225016

Anno Accademico 2017/2018

INDEX

Abstract

In this work a new type of fuel cell is investigated. Using the newest studies in matter made by the SAFCell®, Inc. with the support of the University of Pasadena, in California, a real case study is analysed. The work shows an overview about the current type of existing fuel cell. After it moves through several theoretical studies to discover the nature of the solid acid, a new type of material used to realize the electrolyte of a new kind of fuel cell, called Solid Acid Fuel Cell (or SAFC). The evaluated application is electrical power generation for an isolated house, as a mountain chalet. To get simple and useful the fuel cell methanol is considered as fuel instead of the most common hydrogen. In this way the complexity and the dangerous of the plant are drastically reduce. The new electrolyte permits to work at lower temperature of other cell keeping a high efficiency. The cell is operated under conditions of start-up and steady state to produce an electrical power of 2 kWel. The thermal power of the hydrogen produced by the reformer of methanol is not debated in this work. In the end a comparison between a SAFCell and a Solid Oxide Fuel Cell (SOFC) is made in economical and energy terms.

Any sufficiently advanced technology is indistinguishable from magic.

.

(Arthur C. Clarke)

INTRODUCTION

The increasingly growing energy demand is no longer a problem that can be overlooked. The exploitation of the energy resources that our planet offers us is the first cause of the climatic upheavals that more and more frequently occur. To overcome this, man has researched various forms for the production of energy that could have minimal impact on the environment. One of these is represented by fuel cells. Thanks to these devices it is possible to obtain thermal and electric energy starting from substances such as hydrogen and methane, producing pollutants equal to zero. These are simple chemical reactions of redox, in which the transport of electrons is king. There are many technologies that exploit these mechanisms, but if on the one hand the operation is simple, on the other hand its implementation involves considerable costs. This work was an innovative technology developed by researchers at the University of Pasadena, California, together with the company SAFCell®, Inc. from which the technology took its name. Theorized in the early 2000s and built for less than 10 years, SAFCell are cells that encompass the benefits of various existing technologies today, however, going to have a much lower economic impact with the same efficiency. Based on solid acids, substances capable of modifying their crystal lattice if subjected to certain temperatures, they can represent the fuel cells of the future. By exploiting hydrogen, SAFCell are able to produce energy and simply waste water as a waste product. But hydrogen technology is still scary to many because of the complications that the storage of this fuel requires. As is well known, in fact, in order to have high yields, due to its density, it is necessary to keep the hydrogen in the form of liquid. This involves high cryogenic technologies with consequent associated consumption. However, recent studies have shown that some solid acids can work directly using another fuel: methanol. This fuel in liquid form in ambient conditions greatly simplifies the whole storage and transport phase. Moreover, it does not require a connection to the distribution network, as instead require other fuels, for example methane. It is therefore possible to hypothesize a scenario in which SAFCell can supply isolated and difficult to reach systems, such as alpine shelters, guaranteeing their energy autonomy.

. The task of this discussion is to compare two apparently similar technologies, SOFC and

SAFCell, in this context. The costs and actual consumption will be investigated to guarantee power of the order of 1500 W and then the costs for the construction of the two plants. Given the impossibility of having these two technologies at your fingertips, a computer modeling work takes place. To do this it is necessary to use a suitable simulation program (ASPEN PLUS). Through appropriate research in the available literature, the input parameters have been set both for material flows and for the thermodynamic characteristics of the various components of the plant. In the final phase we will use methodologies to perform an economic analysis based on the methodologies imposed by authoritative texts in the field of analysis, synthesis and capital cost estimation.

TABLES INDEX

FIGURES INDEX

CHAPTER 1: FROM CHEMICALS TO ELECTRIC

1.1 INTRODUCTION

Since ancient times, man has always changed the environment around him to take advantage of it. Deforestation, reclamation, diversion of river courses: all these works have changed the face of the Earth, making it more livable for humans. And yet, nothing has produced the distortions as important as the advent of the Industrial Revolution. It was at that time the balance between Earth and men turned to the latter with dangerous effects.

The use of fossil fuels, massive deforestation and intensive livestock breeding are among the main factors in the production of greenhouse gases, thus feeding global warming. The current world average temperature is 0.85 ° C higher than the levels of the end of the nineteenth century ([1]). According to the greatest experts in global climatology, this increase is mainly caused by the work of man. All this cannot leave us indifferent, because the harmful effects of overheating directly and indirectly affect the human population. Melting glaciers and the related rise in seas, floods and desertification are only some of the consequences of a policy that does not consider the needs that planet Earth possesses

Here, then, is the reason for the birth of treaties such as the Kyoto Protocol or, more recently, the Paris Agreement, aimed at avoiding dangerous climate changes, limiting global warming below 2 ° C. The Paris agreement has introduced several objectives concerning climate and energy:

• by 2030 the 40% cut in greenhouse gas emissions compared to 1990;

• 27% improvement in energy efficiency;

• 27% of the energy needs obtained from renewable sources.

Hence the need not only moral and ecological, but also the policy of finding alternatives to the classic consumption of fossil fuel to produce electricity.

In the last decades many steps have been taken in the study and development of

alternative sources to the classic coal to produce electrical and thermal energy. Wind turbines and solar panels have now entered the common imaginary as synonyms for clean energy and their functioning is known to most of the population.

Another option is given, instead, by the exploitation of the chemical potential of known fuels. The chemical potential can be defined as the property of a mass flow characterized by a high value of the Gibbs free energy. Consider an ideal gas. From the definition of Gibbs free energy, we have:

$$g = h - T * s \tag{1.1}$$

where h is the specific enthalpy, T is the temperature, it is the specific entropy.

You can then find the Gibbs free energy of a mixture in a particular state $g(T,p_i)$ taking into account that:

$$g(T, p_i) = h_i(T, p_i) - T * s_i(T, p_i) \tag{1.2}$$

Enthalpy is a state function that depends only on the T

$$h_i(T, p_i) = h_i(T, p) \tag{1.3}$$

For entropy it need to do some calculations

$$ds = (\frac{ds}{dT})_p dT + (\frac{ds}{dp})_T dp = \frac{cp}{T} dT - \frac{R}{p} dp \tag{1.4}$$

And so you have

$$s_i(T, p) - s_i(T, p_i) = -R \ln \frac{p}{p_i} \rightarrow s_i(T, p_i) = s_i(T, p) + R \ln \frac{p}{p_i} \tag{1.5}$$

From Dalton's Law, under perfect and ideal gas condition, the mola fraction of a component in a mixture is equal to:

$$y_i = \frac{p_i}{p} \tag{1.6}$$

Changing the (1.6) into (1.5) you obtain

$$s_i(T, p_i) = s_i(T, p) + R \ln y_i \tag{1.7}$$

And with simple mathematical operation you arrive to write

$$g_i(T, p_i) = g_i(T, p) + RT \ln \frac{p_i}{p} \tag{1.8}$$

As can be seen, the chemical potential of a mixture depends not only on the temperature of the mixture, but also on the partial pressures of the individual components.

1.2 GALVANIC AND ELECTROLYTC CELL

Generally, three approaches are used to obtain electrical power from chemical energy:

- Thermo-chemical transformation (high temperature heat is produced)
- Thermo-mechanical transformation (mechanical energy is produced at the crankshaft in a thermodynamic cycle)
- Electro-mechanical transformation (electric power is produced in an alternator)

However, these methods are very complex and cannot fully exploit the chemical energy of a substance. In 1839 William Grove was the first to understand how to use the chemical potential of mass flow as much as possible. By studying electrolysis, he understood that electrical energy could be used to divide water into oxygen and hydrogen. He then thought of a method to make the opposite reaction take place. In this way an electrochemical device was born, able to directly convert the energy deriving from a chemical reaction into electrical energy, that is the first

electrochemical cells.

The structure of an electrochemical cell is very simple (Fig. 1.1), three main layers with different tasks from each other:

- an electrode in which oxidation reactions take place called an anode
- an electrode in which the reduction reactions called the cathode take place
- a layer that physically separates these two layers called the electrolyte.

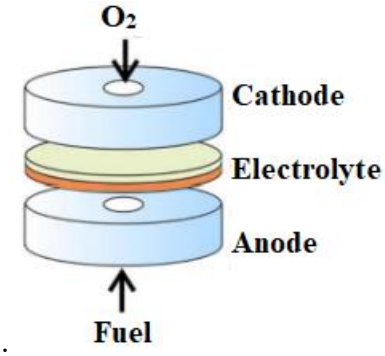

Fig 1.3- Structrure of an electro-chemical cell

The anode is the layer where the reaction of oxidation happens, i.e. in which there is a reaction with liberation of electrons.

$R_1 \leftrightarrow X_x + e^-$

In the cathode happens the reduction reaction, and electrons reacting with elements are here allow the products formation.

$R_2 + X_x + e^- \leftrightarrow P$

Total reaction (redox) could be descripted by

$R_1 + R_2 \rightarrow P$

The electrolyte physically separates the anode and the cathode and must be characterized by low molecular diffusivity, low ability to conduct electrons and high ability to conduct ions. Even if there is no contact between the two reagents, the reaction occurs because at the equilibrium, under the pressure of the chemical potential, the protons migrate from the anode to the cathode. Since the electrolyte does not allow the passage of electrons, they accumulate at the interface forming an electrical double layer, also called Gouy-Chapman layer[([2])].
At the same time the ions, which can travel through the electrolyte, are deposited on the cathode, forming a further double layer, but with opposite sign. This creates a potential difference ΔV between the two electrodes. The electrons, however, not being able to cross the electrolyte, need an external circuit in which to move and thus create an electric current I. The presence of an electric current and a potential difference produces an electric power

$$W_{el} = \Delta V * I \tag{1.9}$$

The conversion of chemical energy to electrical energy can occur through a spontaneous or non-spontaneous reaction. The spontaneity of a reaction can be determined by exploiting the chemical potential difference, i.e. ΔG.
As seen in (1.8) this quantity depends on the partial pressures of the substances taking part in the reaction. An additional formula can then be written to calculate the variation of Gibbs free energy of formation considering the free Gibbs energies of the reagents and products.

$$\Delta g_f = g_{f(product)} - g_{f(reactant)} \tag{1.10}$$

as example for hydrogen combustion

$$H_2 + \frac{1}{2}\, O_2 \rightarrow\ H_2O$$

the Equation (1.10) becomes

$$\Delta g_f = g_{f(H_2O)} - g_{f(H_2)} - \frac{1}{2} g_{f(O_2)}$$

If ΔG<0 the reaction will be spontaneous and we are talking about galvanic cells, i.e. cells in which the chemical potential of a substance is transformed directly into electrical energy; if ΔG>0 the reaction will be non-spontaneous and we talk about electrolytic cells. An electrolyte cell contains an electrolyte that allows to produce chemicals by means of electric current. The best-known case is that of oxygen and hydrogen production starting from water electrolysis.

$$H_2O \rightarrow H_2 + \frac{1}{2}\, O_2$$

1.3 FARADAY'S LAW

If we consider the (1.8) as reversible, then all the Gibbs free energy is converted into electrical energy. Gibbs free energy can then be used to find the open circuit voltage (OCV) of a galvanic cell. It is indicated with q_{e-} electron charge (equal to 1,602e^{-19} coulomb) and we could write

$$1\ molecule\ H_2 \rightarrow 2\ q_e{-}$$

Because in the reaction we obtain 2 electrons.
From Avogadro's Law we know that

$$1\ mole\ H_2 \rightarrow\ N_A\ molecule\ H_2 \rightarrow\ \ 2\ q_e{-} * N_A \rightarrow 2\ F$$

with N_A it is indicated the Avogadro's number, equal to 6.022e23 [mol^{-1}] and with F the Faraday's constant (96487 C/mol).
The value just obtained is multiplied for the flow rate and the current produced is thus

obtained

$$I = 2 * F * n_{H_2} \quad (1.11)$$

Faraday's law is precisely the relationship between the molar flow rate of a species to the electrodes (n_R), the intensity of current flowing in the external circuit (I) and the charge number of the chemical species z_R.

$$n_{H_2} = \frac{I}{z_R * F} \quad (1.12)$$

In a fuel cell the electrolytes must be good ion conductors and be impermeable to electrons. The most relevant conductivity is therefore that of the ionic type. It can be defined by the formula

$$\sigma_{ionic} = F^2 * {z_{ionic}}^2 \, u_{ionic} * C_{ionic} \quad (1.13)$$

in which z_{ionic} is the ionic charge number, u_{ionic} is ionic mobility, the ratio between the ion velocity and the unit electric field, and C_{ionic} it is the concentration of ions in the electrolyte structure. The principle of conservation of the charge is valid in the cell, ie the electric current must be equal to the ionic current. From the measurements carried out we have seen that the electronic conductivity σ_e it is six orders of magnitude greater than the ionic one. Remembering that the conductivity is the inverse of the resistance, then the ohmic fall can be written

$$\Delta V_{electrolyte} = \frac{I_{ion}}{\sigma_{ion}}$$

$$\Delta V_{circuit} = \frac{I_e}{\sigma_e}$$

For what has been said up to now it is easy to see that $\Delta V_{elettrolita} >> \Delta V_{circuito}$ and therefore the falls in the electrolyte are very large, which is why we tend to reduce the thickness to a minimum.

1.4 THERMODYNAMIC OF THE ELECTRO-CHEMICAL CELL

You consider the cell as a black box in which only the input and output data are known (Fig. 1.2).

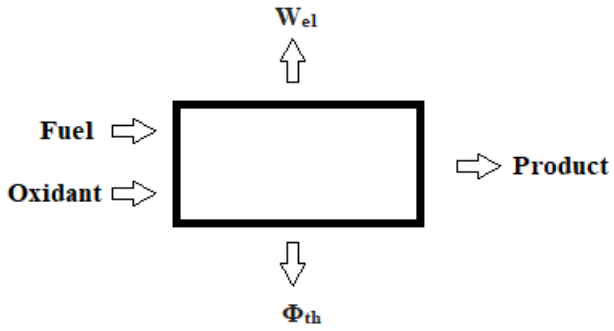

Fig. 1.2 - Input and output in a electro-chemical cell

It is hypothesized that the cell is of the galvanic type, that it works in stationary conditions and that the reactions occurring inside it are reversible. The first and second principles of thermodynamics are applied to the cell

I) $q - l_{el}^{R} = \Delta h_{react}$

II) $\frac{q}{T} = \Delta s_{react}$

And we obtain

$$l_{el}^{R} = -\Delta h_{react} + T * \Delta s_{react} = -\Delta g_{react} \qquad (1.14)$$

Reversible electric work can also be obtained in another way

$$l_{el}^{R} = \frac{W_{el}^{R}}{n_{fuel}} \tag{1.15}$$

and by applying the Faraday law we have

$$l_{el}^{R} = \frac{(I * V)^{R}}{\frac{I}{z_{fuel} * F}}$$

The two equations just found for reversible electric work are equalized and obtained

$$V = \frac{-\Delta g_{react}}{z_{fuel} * F} \tag{1.16}$$

The voltage measured in a cell when the circuit is open, i.e. I = 0, is called open circuit voltage (OCV). The OCV depends only on Δg and on z_{fuel}. The latter depends on the type of reaction, and specifically on the type of fuel, while the parameter Δg it is a function of temperature and pressure. Therefore, the OCV will also depend on these two parameters. An increase in temperature produces a reduction of Δg with consequent decrease of the OCV.

Moreover, we could note that

$$OCV = \frac{-\Delta g}{z_{fuel} * F} = \frac{-\Delta g_0}{z_{fuel} * F} + \frac{RT}{z_{fuel}} \ln \frac{\prod^{R} \frac{p_i}{p_o}^{\nu_i}}{\prod^{P} \frac{p_i}{p_o}^{\nu_i}} \tag{1.17}$$

This equation is called the Nernst equation. In order to have a larger OCV, the partial pressure must therefore be increased p_i^R of the reagents or decrease that of the products p_i^P.

1.4.1 POLARISATION CURVES

As we have seen, the OCV is the maximum voltage that is generated by a redox reaction and corresponds to the voltage that would be measured if there were no losses. When the circuit is closed, a non-zero current I begins to flow in the external circuit, breaking the chemical equilibrium to the electrodes. The system is no longer in ideal conditions and the potential drop in the cell will always be lower than the OCV. This difference is due to phenomena such as mass and charge transport. The relation between the potential drop and the current intensity is called polarisation curve.

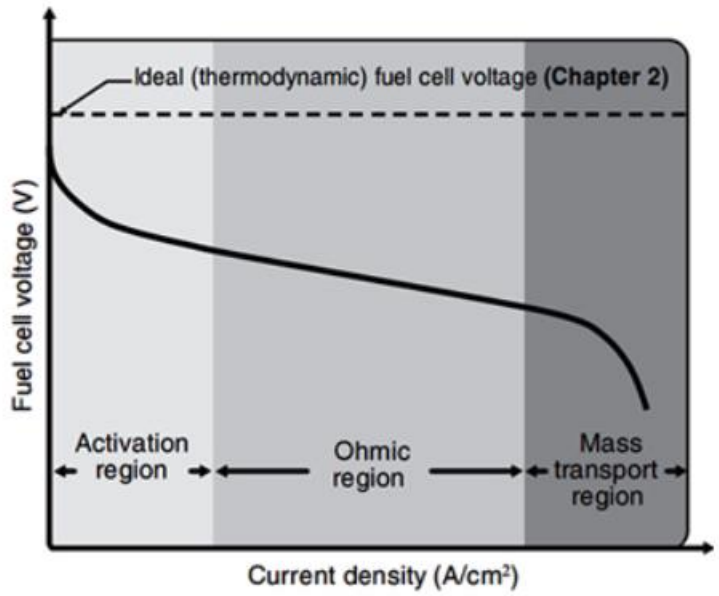

Figura 1.3- Polarization curve for a galvanic cell

From Fig 1.3 it is noted that the curve can be divided into three zones and in each of them a particular phenomenon prevails. In the first zone the charge transfer prevails, that is a kinetic process connected to the activation of the electro-chemical reaction to the electrodes. Activation represents the energy barrier that must be overcome in order for the reaction to take place. It is related to the speed of electrolyte reactions and the associated loss is expressed by the Tafel equation:

$$\eta_{act} = \frac{RT}{\alpha nF} \ln \frac{i}{i_0} \quad (1.18)$$

where α is the charge transfer coefficient and i_0 is the exchange current density. In the second zone the charge conduction prevails, that is the phenomenon of the transport of electrons and ions, to which the ohmic losses are associated. The ohmic drop of potential can be expressed by the formula

$$\eta_{ohm} = RI = \rho \frac{L}{A} i = ASR\ i \quad (1.19)$$

The product between the resistivity ρ and the thickness of the electrolyte L takes the name of Area Specific Resistance (ASR). The ASR of the components should be smaller of 0.5 ohm*cm^2 (ideal =0.1), to guarantee a high-power density with a target of 1kW/dm^3 e 1 kW/kg. High power density is necessary to reduce costs by minimizing the amount of material per kW. The need to minimize cell resistivity has a major impact on the selection and processing of cell components. For low temperatures, the introduction of hydrophobic polytetrafluoroethylene 40 years ago simplified the production of porous structures, which held liquids and allowed the diffusion of gas. A further step forward was the insertion of metal micro-particles (usually platinum Pt) which had the task of acting as a catalyst. The last area is characterized by mass transport, or diffusion. Molecular diffusion is a process that affects the number of reagents at a given point in the reaction, determining the concentration of reagents at one point of the electrode. It can be calculated using the formula

$$D_j^{eff} = (\frac{\varepsilon}{\tau})^n * D_j \quad (1.20)$$

Where D_j^{eff} it is the effective diffusion coefficient, D_j is the diffusion coefficient of the j-th species, ε is the porosity, τ the tortuosity and n is the shape parameter. Diffusion does not directly cause a potential fall, but a reduction in the concentration of the reactants produces a decrease in potential due to the Nernst

law.

The polarisation curve expresses the relationship between the potential across the V_c electrodes and the current density that passes through the cell. This relationship therefore depends on the OCV and on the different losses due to several factors (activation, diffusive, ohmic).

$$V_c(T,p,i) = OCV(T,p) - \eta_{act}(i) - \eta_{ohm}(i) - \eta_{diff}(i) \quad (1.21)$$

1.4.2 THERMAL FLUX

During its operation, the cell exchanges thermal flows with the outside. These flows are generated by the reaction itself and by overvoltage. In a galvanic cell one speaks of exotherm behavior in which $\Phi_{th}<0$.

The flux Φ_{th} it is in turn formed by the contribution of two flows, the one due to the reaction and the one that is attributed to the irreversibility of the overvoltage effects.

$$|\Phi_{th}| = |\Phi_{react}| + |\Phi_{irr}| \quad (1.22)$$

The heat produced by the reaction can be calculated as follows:

$$q_{react} = T * \Delta s \rightarrow \Phi_{react} = q_{react} * n_f \rightarrow \Phi_{react} = \frac{T*\Delta s}{z_f*F*I} \rightarrow$$

$$|\Phi_{react}| = -\frac{T*\Delta s}{z_f*F*I} \quad (1.23)$$

the heat produced by transport phenomena can be calculated

$$\Phi_{irr} = -I * \sum \eta_i \rightarrow |\Phi_{irr}| = I * \sum \eta_i \quad (1.24)$$

Combining (1.22) with (1.24) we obtain

$$|\Phi_{th}| = -\frac{T*\Delta s}{z_f*F*I} + I*\sum\eta_i = \left(\frac{-\Delta h+\Delta g}{z_f*F} + \sum\eta_i\right)*I = \left(-\frac{\Delta h}{z_f*F} - V_c\right)*I \quad (1.25)$$

The initial chemical energy is divided into thermal energy and electrical energy. In the case one considers an ideal security in electric energy

$$V_c = -\frac{\Delta h}{z_f * F} \rightarrow \Phi_{th} = 0$$

In the real case, however, there will be entropy generation due to both the transport phenomena and the reaction itself. The thermal power increases linearly with the current I. The higher the current I will be, the greater will be the associated V_c which causes further heat production.

1.5 OPEN CIRCUITS AND CLOSED CIRCUITS

Galvanic cells can be classified into closed systems and open systems. In closed systems the reaction is powered by the molecules that make up the electrodes and do not require external power supply. In open systems, the reaction occurs between the reagent molecules that are continuously supplied to the system thanks to a mass flow coming from the outside, while the materials that make up the electrodes do not participate in the reaction. We speak in the first case of batteries, while in the second case we will have fuel cells.

1.5.1 BATTERIES

The batteries are electrochemical cells that operate as a closed system. They can work both directly (from $\Delta G \rightarrow W_{el}$) or discharge phase, both inversely (from $W_{el} \rightarrow \Delta G$) said charge phase. The most famous batteries are those with lithium-ion, used in many fields, especially in the electronic one. These batteries have the advantage of being very light, a factor attributable to the charge density of very high Li ions. They also do not suffer from the memory effect and therefore do not undergo hysteresis processes which reduce its efficiency. However, they suffer from progressive degradation even without effective use. In other words, they have a fixed lifespan that does not depend on the number of charge / discharge cycles. In the discharge phase the reaction that occurs in a lithium battery is:

Anode: $Li_xC_6 \rightarrow 6C + (x)Li^+ + (x)e^-$

Cathode: $Li_{1-x}MO_2 + (x)Li^+ + (x)e^- \rightarrow LiMO_2$

Total: $Li_xC_6 + Li_{1-x}MO_2 \rightarrow 6C + LiMO_2$

in which M is a reducing metal (e.g. cobalt Co).
In a charged battery if the circuit is open, the lithium atoms in the anode are in equilibrium with the Li + ions present in the electrolyte. When the circuit closes, due to a resistance, for example, the balance breaks and the ions start traveling from the anode to the cathode: it is the discharge process. First, the ions of the anode traveling are those closest to the electrolyte, which occupy the sites available in the cathode structure. As the process continues, all the atoms in the anode participate in the reaction, and when the last site of the cathode has been occupied the process is interrupted: the battery is empty.
The reverse process is then carried out in such a way as to re-establish the chemical potential that was present in the battery first, thereby carrying out a charging process.

Lithium-ion batteries have a nominal voltage V_c of about 3.6-3.7 V. This value is not only influenced by transport phenomena, but also by thermodynamic ones. In fact, the quantity of lithium at the anode depends on the operating temperature. Other parameters that characterize a battery are:

- the capacity C measured in amperes per hour [Ah], which is related to the availability of electrode sites to accommodate the ions
- stored energyE [Wh] which depends on the nanostructure of the electrode materials, their surface and the number of cells in the stack. It can be calculated with the formula

$$E = n * V_c * C \tag{1.25}$$

1.6 FUEL CELLS

A fuel cell (FC) is an electrochemical reactor in which a redox reaction occurs producing electrical power and thermal power. Generally, the reaction that occurs inside it involves hydrogen and oxygen with the consequent production of water

.

$2H_2+O_2 \leftrightarrow H_2O$

They are defined as a clean technology, free from pollution. By not operating with a thermal cycle, as is the case with internal combustion engines, their efficiency is not limited by the efficiency of Carnot. This does not mean that fuel cells are more efficient than those of the more classic internal engines, but that it is calculated in a completely different way. In fact, it is equal to the maximum amount of electrical power that can be obtained from a given fuel flow.

$$\eta_{el} = \frac{W_{el}}{G_{el} * LHV_{fuel}} \tag{1.26}$$

The advantages of using these cells are high efficiency, modularity, low emissions of NO_x e SO_x and possibility of cogeneration.

The oxidation reaction at the anode makes it possible to free the electrons which, by crossing an external circuit, produce electrical energy, arrive at the cathode and participate in the reduction reaction. In addition to the production of electricity and such products H_2O (and CO_2 if hydrocarbons or alcohols are used), fuel cells also produce heat. The applications of fuel cells are the most varied. It goes from the domestic use for smaller power plants, to the automotive sector for powers ranging from 1kW to 100kW, up to the distribution on the electricity grid for large power plants. The power density produced by the fuel cells is greater than that produced by the batteries and, unlike the latter, the fuel cells have the advantage of not having to recharge. For their operation, just send the fuel to the cell itself. In addition, they can be used in cogeneration systems, as exhaust gases escaping from the Fuel Cell can be sent to a turbine to produce additional energy, increasing the efficiency of the system by up to 80%. Not needing a charge phase, they can produce electricity if the fuel is supplied. Moreover, it has been seen that a fuel cell releases much less pollutants into the atmosphere than those introduced by the common electricity production systems. The values of about 4 ppm of CO are reached and less than 1 ppm of NO_x, reducing the quantity entered by one (in the case of NO_x) or more orders of magnitude (case CO). Also, the sound factor should not be underestimated. A fuel cell produces about zero noise pollution, since the conversion of energy through the chemical reaction is virtually silent. Nowadays this technology is still growing, mainly due to some problems, which make it less competitive for the market. These problems include the very high initial cost of maintenance, around 1200 euros / kW, and the lack of familiarity with the fuel cell industry. Many governments have therefore invested in research, wanting to reduce costs and bring them to more acceptable values, such as 400 €/kW. Further investments have been allocated with the aim of "educating" the industries, to make this technology better known and more familiar to large companies that deal with energy production. Even the average user must become familiar with this technology, to acquire the knowledge that can overcome concerns in terms of safety, due to the presence of hydrogen, management costs, reliability and maintenance.

1.7 HOW IS MADE A FUEL CELL

In general, a fuel cell is made up of several layers, of different materials superimposed on one another, with different purposes. In Fig. 1.4 you can see an exploded view of the cell.

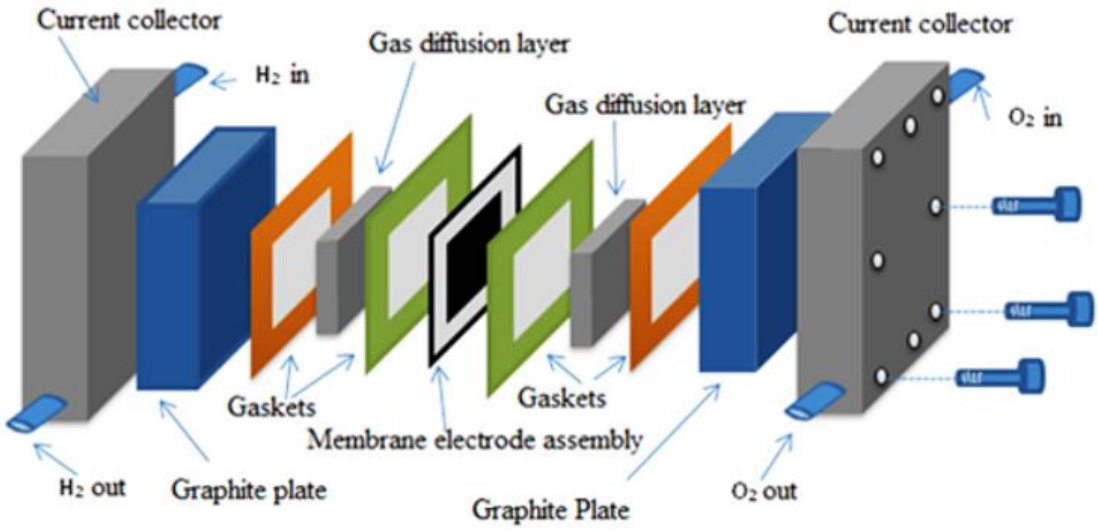

Fig 1.4- Layers of a fuel cell

The heart of the cell is formed by the membrane electrode assembly (MEA), formed by the electrolyte and the catalyst layers (anode and cathode). It is in this part of the cell that electric power is produced. On the two sides of the MEA is the gas diffusion layer (GDL). It is generally composed of a carbon sheet in which the carbon fibers are partially coated with hydrophobic materials such as polytetrafluoroethylene (PTFE). Its function is to transport the fuel or products from the channels present on the bipolar plate to the reaction sites, electrically connecting the electrodes to the external circuit. GDL is generally porous, allowing gas to pass through it quickly. To prevent gas and / or fluid leaks, an additional layer called gasket is placed, generally composed of gum-like

polymers. Each MEA produces about 1.2 V in the typical conditions of use (T = 25 ° C, p = 1 bar). This value is too low to produce a significant amount of power. Hence the need to stack the cells in series in such a way as to increase the equivalent produced tension. The various MEAs are connected to each other by two bipolar plates. These plates are composed of metals, carbon (generally graphite) and composite materials and are also responsible for the distribution of fuel and the removal of redox reaction products (e.g. water). This is made possible by small channels present on the surface of the plates that in addition to allowing the refueling of fuel can also be crossed by cooling fluids. For these reasons the bipolar plates must be excellent electrical conductors and prevent molecular diffusion.

1.8 CLASSIFICATION AND TEMPERATURE RANGE

You can make a classification of existing fuel cells today by adopting different criteria. The first classification is a function of the material that makes up the electrolyte. We therefore speak of alkaline fuel cells (AFC), polymer electrolyte membrane (PEMFC) cells, phosphoric acid cells (PAFC), molten carbonate fuel cells (MCFC) and solid oxide cells (SOFC). Each cell has its own chemistry and therefore uses one fuel or another. AFC, PEMFC and PAFC essentially exploit pure hydrogen which is sent to the anode, while MCFC and SOFC operating at higher temperatures are more tolerant and can exploit different hydrocarbons as fuel. All this can be summarized in Fig. 1.5

You can make a classification of existing fuel cells today by adopting different criteria. The first classification is a function of the material that makes up the electrolyte. We therefore speak of alkaline fuel cells (AFC), polymer electrolyte membrane (PEMFC) cells, phosphoric acid cells (PAFC), molten carbonate fuel cells (MCFC) and solid oxide cells (SOFC). Each cell has its own chemistry and therefore

uses one fuel or another. AFC, PEMFC and PAFC essentially exploit pure hydrogen which is sent to the anode, while MCFC and SOFC operating at higher temperatures are more tolerant and can exploit different hydrocarbons as fuel. All this can be summarized in Fig. 1.5.

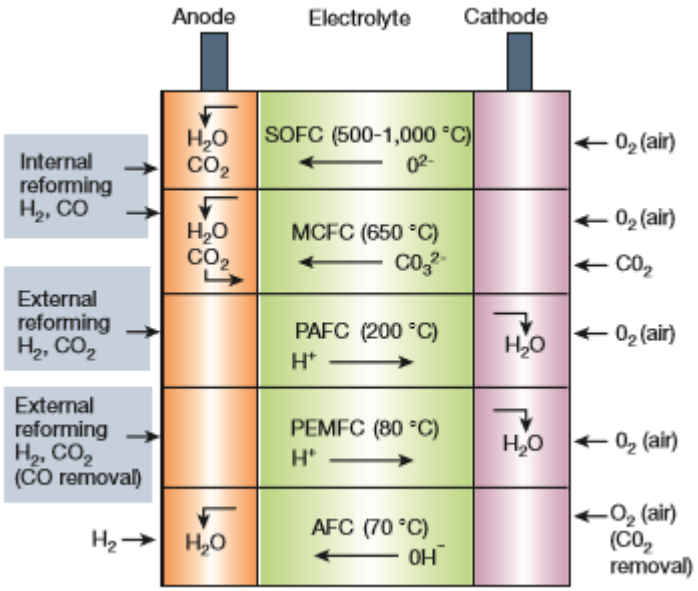

Fig. 1.5- Summary of fuel cell types

The use of hydrogen or hydrocarbons also affects the overall efficiency of the plant. Although its technology is in a phase of considerable development, the production and storage of pure hydrogen meet both technical and economic obstacles, which cause a reduction in system efficiency. From Fig 1.6 this is quite clear.

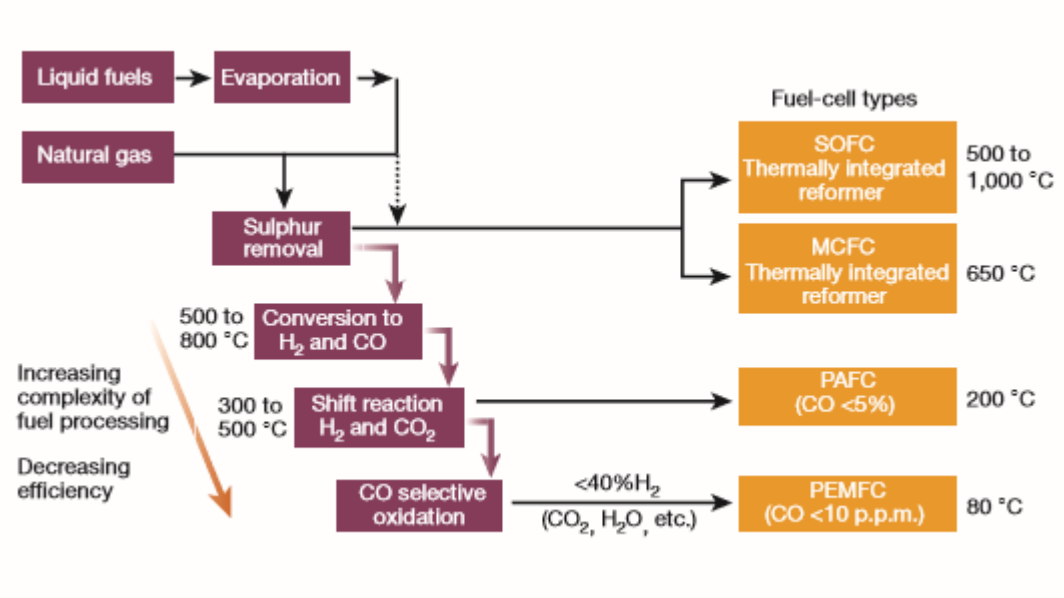

Fig 1.6- Fuel cell types and fuel processing

The use of external fuel processors (reformers), which also use fuel, increase the complexity of the system to the detriment of global efficiency.

Another classification can be determined by the ions that the electrolyte allows to exchange. In fact, there are cells that allow the exchange of ions O^{2-} (SOFC, MCFC, AFC) and cells in which the exchanged ions are H^{+} (PEMFC, PAFC).

From all this it is evident that for certain technical specifications correspond different types of fuel cells. A further factor of a certain importance is given by the operating temperatures of the various cells. It goes from cells to low temperatures (DMFC, AFC and PEMFC). At medium temperature (PAFC), f to reach cells that work at temperatures of about 500 ° C (MCFC and SOFC).

1.9 PEMFC

The polymer membrane fuel cell (PEMFC) was the first to be developed by General Electric in the 1960s. It has an efficiency of over 50% and a very low environmental

impact. It consists of a positively charged electrode (cathode) where oxygen is reduced by reacting with the ions H^+ producing water and heat, and a negatively charged electrode (anode) in which the present hydrogen is oxidized producing ions H^+ and electrons, as shown in Fig. 1.7

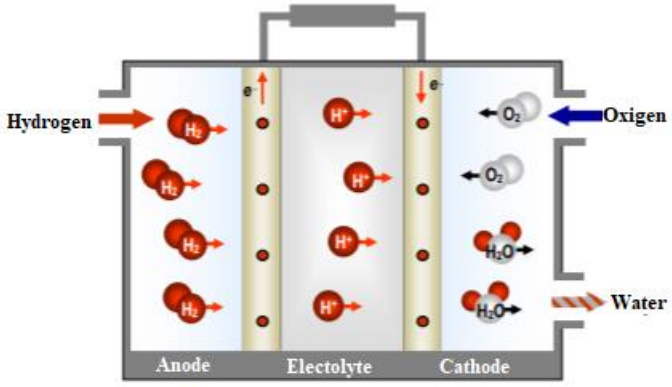

Fig 1.7- PEMFC

The reactions that take place in a PEMFC are:

Anode: $2H_2 \rightarrow 4H^+ + 4e^-$

Cathode: $O_2 + 4e^- + 4H^+ \rightarrow 2H_2O$

Total: $2H_2 + O_2 \rightarrow 2H_2O$

with an OCV = 1.18 V. Because this value is really low, mass cell stacks are used to produce significant power. Therefore, the total electric power produced is given by:

$$W_{el} = n_c * V_c * I \qquad (1.27)$$

The electrolyte is composed of a polymer, NAFION®. The starting point for NAFION® is polyethylene $(CH_2)_n$, from which a matrix called polytetrafluoroethylene or PTFE is obtained through a perfluorination process. The

PTFE is finally sulphonated with the acid HSO_3 to get the NAFION. Thanks to the strong bond between fluorine and carbon, it is very resistant to chemical attacks over time. Furthermore, the polymer is strongly hydrophobic, thus favoring the escape of water from the cell. The presence of ions SO_3^-(hydrophilic) in a hydrophobic structure makes possible a phenomenon of ion transport H^+ known as hopping. However, this process is only possible if the membrane remains moist. Therefore, the operating temperature of the cell must be such as to allow the presence of water in the liquid state and at the ambient pressure. For this reason, the operating range of a PEMFC never goes above 100 ° C. These temperatures are however too low to trigger the electrochemical reaction in the cell and this explains why it is necessary to introduce a catalyst, usually platinum.

The introduction of a catalyst like Pt, however, involves two major disadvantages: the first lies in the cost of the material itself and the second in the fact that the Pt suffers from a phenomenon called poisoning. If for the first one has managed with time to find a solution (0.5 mg/cm^2 of Pt is enough to trigger the reaction), for the second problem the question is still open today. For temperatures below 150 ° C, in fact, platinum binds strongly with carbon monoxide, reducing the areas useful for electrochemical reactions. From the tests carried out in the laboratory it has come out that a carbon concentration of 10 ppm in the fuel is already sufficient to affect the performance of the catalyst making it inefficient. Therefore, only hydrogen is used for PEMFCs. However, the polymeric membranes have a high proton conductivity, ensured by the acidic ionic groups (SO_3H) which depend on the degree of sulfonation and the thickness of the membrane, good mechanical, thermal and chemical resistance, low gaseous permeability depending on the thickness of the membrane itself. Yes, a certain speed of cold start, order of a few minutes.

1.10 SOFC

Solid-acid fuel cells (SOFCs) are cells that use a solid-state electrolyte and reach the highest temperatures among all types of fuel cells. The electrolyte used is a YSZ

ceramic material (zirconia stabilized with ittria) which conducts ions O_2^-. he electrolyte is abundantly present in nature, is not toxic and is also economical. However, it has some drawbacks due to the high coefficient of thermal expansion.

The anode is made of cermet, which is a ceramic and metal composite material that also acts as a catalyst for the internal reforming reaction.

The cathode is composed of a composite ceramic material, in which electron conducting oxides and ion-conducting ceramic materials are present. Typically, some composites are used that take the name of perovskite. The perovskites have the formula ABO_3, where A is a rare earth and B is a transition metal. Perovskite has a cubic structure in which vertices are inserted atoms A, in the center the atom B and O occupies the center of each face (Fig.1.8)

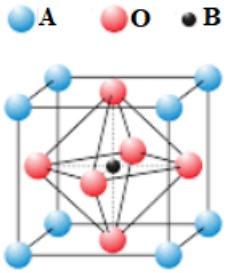

Fig 1.8- Perovskite's atomic distribution

Nowadays the most used perovskite is lanthanum-strontium-manganese (LSM).

The reactions that take place in the electrodes are

Anode: $2H_2+2O_2^- \rightarrow 2H_2O+4e^-$

Cathode: $O_2+4e^- \rightarrow 2O_2^-$

Total: $2H_2+O_2 \rightarrow 2H_2O$

From Fig. 1.9 it is possible to see how the ion passes from the cathode to the anode.

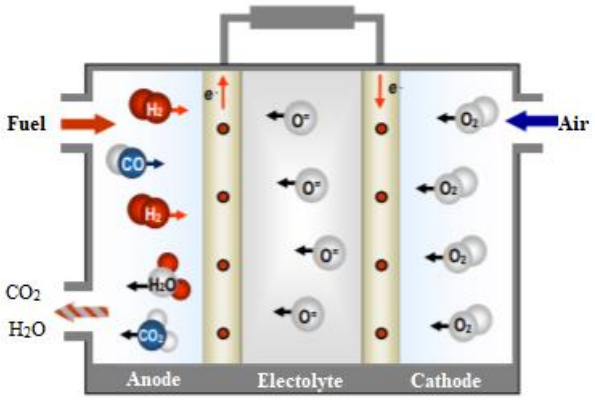

Fig 1.9- SOFC

The presence of a ceramic material allows to reach temperatures of 600-800 ° C and at these temperatures there is an improvement in the kinetics of the electrochemical reaction, in the diffusion of the reagents in the electrode and the ohmic falls are limited. All this guarantees a high efficiency (about 56%), higher than that which occurs in a PEMFC.

Another advantage of using SOFCs is the flexibility in the choice of the fuel to be used. The high temperatures achieved in fact allow the direct use of hydrocarbons, since there is no need for a high-quality catalyst as in the case of PEMFCs. Although the hydrogen reaction remains the fastest kinetic reaction, it is not uncommon to find methane or carbon monoxide as fuel in SOFCs.

In order for these fuels to be used, some processes to convert them must be implemented. We are talking about Steam Methan Reforming (SMR) and Water Gas Shift (WGS).

The former allows to obtain hydrogen and carbon monoxide from methane

SMR: $CH_4+H_2O \rightarrow 3H_2+CO$

The reforming reaction can take place directly in the anode or in a separate reformer but in any case, integrated into the SOFC stack. The internal conversion of hydrocarbons increases the overall efficiency of the system. The second reaction allows instead to exploit the carbon monoxide of SMR to obtain H_2

WGS: $CO+H_2O \rightarrow H_2+CO_2$

Obviously, the starting hydrocarbon can be chosen from a wide range. The most used, for economic and transport needs, is still natural gas, which may contain traces of impurities. Among these the most dangerous for the operation of the cell itself is sulfur. 10 ppm of sulfur can damage the cell's anode, while 100 ppm can destroy it in less than an hour of operation. For this reason, they are applied to the fuel before introducing it into the sulfur removal treatment cell.

1.11 OTHER TYPE

The fused carbonate cells (MCFC) are cells that exploit an electrolyte formed by molten carbonate salts suspended in an inert, porous matrix and made in BASE (beta - aluminium solid electrolite). The commonly used salts include lithium carbonate, potassium carbonate and sodium carbonate. These FCs allow the passage of ions CO_3^{2-}(see Fig. 1.10).

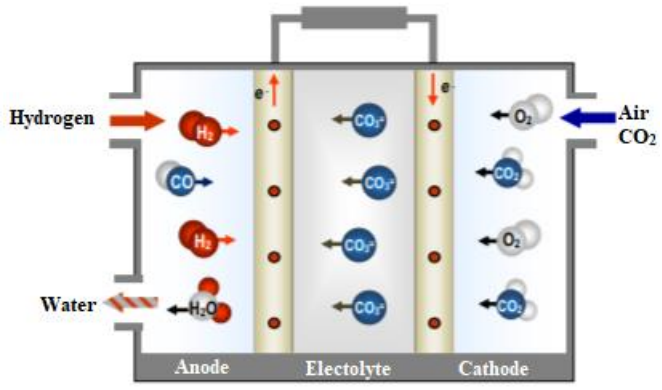

Fig 1.10- MCFC

They operate at a temperature of about 650 ° C and therefore do not require a strong catalyst metal. The high temperatures also reduce the sensitivity to carbon dioxide,

allowing the MCFC to be able to use a wide range of fuels, including natural gas, without the contribution of external reformers. In general, the anode is made of a Ni-Cr alloy and the NiO-doped nickel-oxide cathode. The reduction oxide reactions that occur in the cell are:

Anode: $2H_2+2CO_3^{2-} \rightarrow 2H_2O + 2CO_2 + 4e^-$

Cathode: $O_2 + 2CO_2 + 4e^- \rightarrow 2CO_3^{2-}$

Total: $2H_2+ O_2 \rightarrow 2H_2O$

The main disadvantages of this type of cells are due to the use of a liquid rather than solid electrolyte and to the refill CO_2 from the exhausted anode to the cathode, which complicates the budget of the implant. From a structural point of view, there are two components that compromise efficiency: -in the absence of fuel, during the cooling phase, the Ni-Cr anode needs to be protected from oxidation by introducing an inert gas; - the matrix is resistant to about 3-5 thermal cycles that cross the melting point of the electrolyte salt. The alkaline fuel cells (AFC) use KOH potassium hydroxide as electrolytes and operate at temperatures of 100 ° C. The fuel used is pure hydrogen and a "scrubbing" operation is carried out at the cathode to eliminate carbon dioxide, since in the presence of CO_2 in the reactants the KOH is converted into potassium carbonate K_2CO_3. The electrolyte allows the passage of ions OH^- from cathode to anode (Fig 1.11)

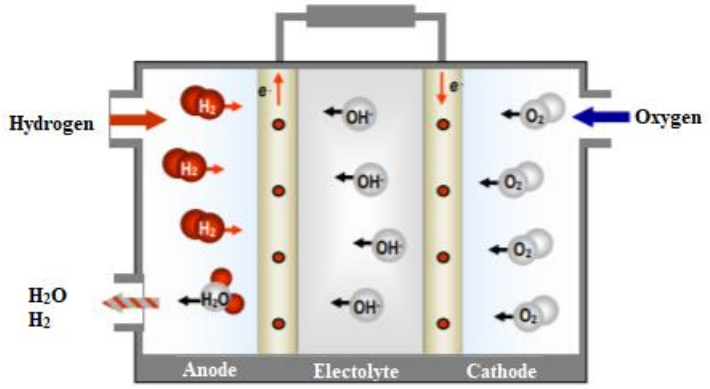

Fig 1.11- AFC

Anode: $2H_2+4OH^- \rightarrow 4H_2O + 4e^-$

Cathode: $O_2 + 2H_2O + 4e^- \rightarrow 4OH^-$

Total: $2H_2 + O_2 \rightarrow 2H_2O$

Despite this drawback, AFCs are the most cost-effective to construct, since the electrode does not require precious materials.

Fuel cells with phosphoric acid (PAFC) are very similar to PEMFCs and also carry ions H^+(Fig 1.12).

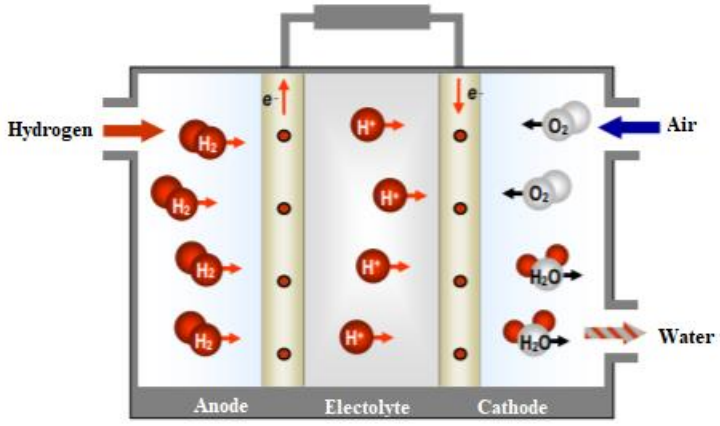

Fig 1.12- PAFC

The electrolyte is formed from the phosphoric acid in the liquid state, because it is the only inorganic acid that satisfies the requirements of thermal, chemical and electrochemical stability while remaining non-volatile. Phosphoric acid does not react with CO2 to form carbonates, as in the case of AFCs, so there are few restrictions on the fuel to be used. The electrodes consist of carbon paper coated with finely dispersed platinum, from which the higher production costs derive. Since phosphoric acid solidifies at 40 ° C, these cells must have some problems in the ignition phase and continuous operation is imposed on them. A further disadvantage is the chemically aggressive electrolyte. The operating temperature is around 150 ° C and 200 ° C.

Anode: $2H_2 \rightarrow 4H^+ + 4e^-$

Cathode: $O_2 + 4H^+ + 4e^- \rightarrow 2H_2O$

Total: $2H_2 + O_2 \rightarrow 2H_2O$

CHAPTER 2: SAFCell

2.1 WHAT ARE ACID SOLID AND THEIR PROPERTIES

Solid acids are compounds whose properties are intermediate between those of a normal acid, such as H_2SO_4, and a normal salt, like Cs_2SO_4. They are formed by an anion of the type XO_4, where X is a pycogen (P, As) or a calcogen (S, Se) that binds to oxygen by means of a hydrogen bond of the tetrahedral type, and a metallic-alkaline cation, which provides for the charge balancing of the hydrogen bonds of all the molecule ([3]). Solid acids are generally not considered for applications because they are soluble in water; moreover, the materials are difficult to process and have very poor mechanical properties (similar to those of the cooking salt) at room temperature. In recent years, however, they have stimulated the curiosity of researchers for some of their curious properties. Many solid acids have a well-ordered structure at room temperature, but if heat is administered it becomes disordered. A typical example is shown in Fig 2.1, where we see how the CsH_2PO_4 steps from a monoclinic structure (characterized by having a single binary axis and a single plane of symmetry) to a tetragonal structure at 228 ° C ([4]).

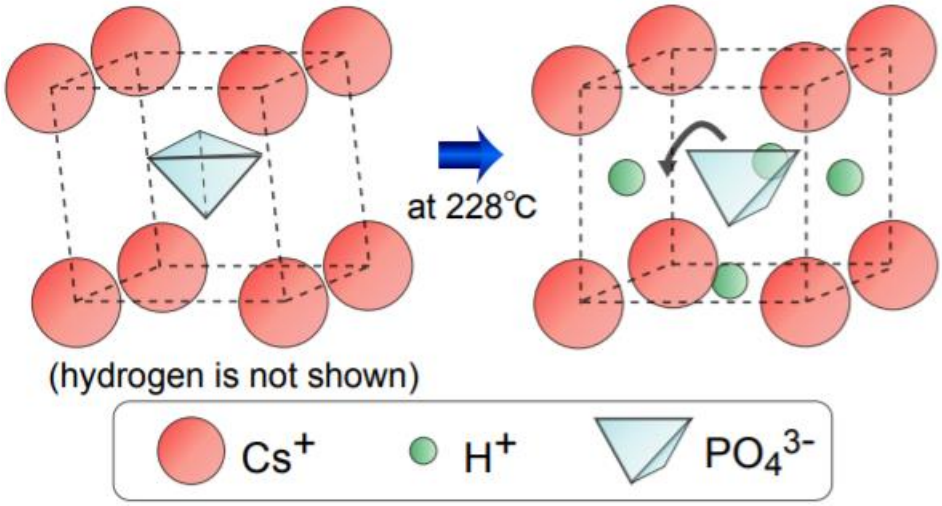

Fig 4.1- Superprotonic transition in a CsH_2PO_4 molecule

The change of structure is accompanied by an increase in protonic conductivity of two or even three orders of magnitude, reaching values of about 10^{-2} ohm^{-1} cm^{-1}. This increase is generally referred to as the "superprotonic phase" ([5]). From Fig 2.2 you can see the conductivity of a solid acid (CsH_2PO_4) compared to that of a more classic polymer used for fuel cells (NAFION ®). The peak that occurs concurrently with the change in structure that leads to a considerable increase in conductivity at temperatures of about 250 ° C is relevant.

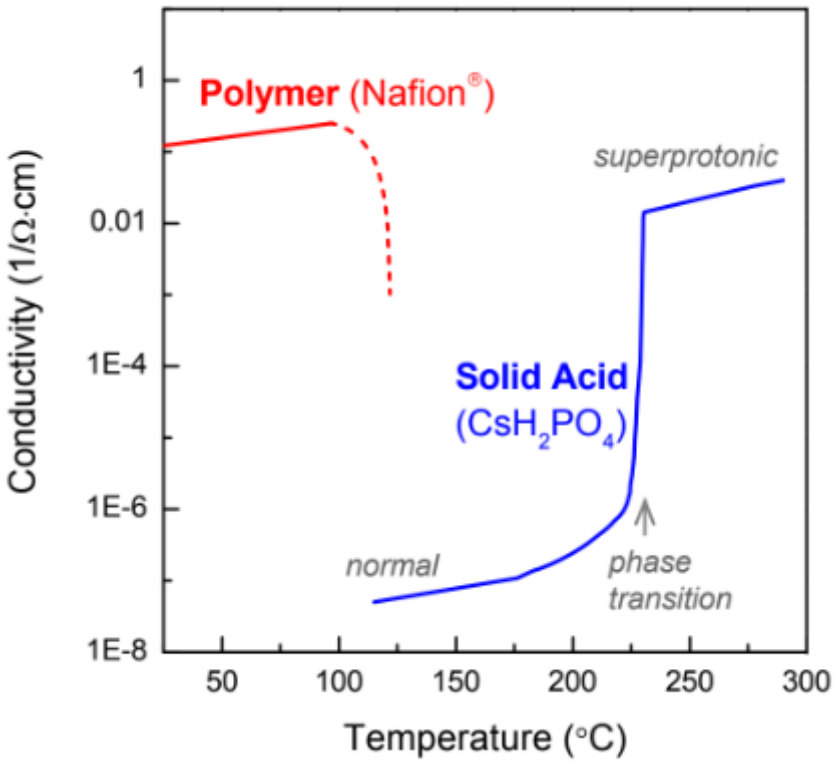

Fig 2.2- Comparision between polymer and solid acid conductivity

2.2 SOLID ACID IN FUEL CELL

In 2001, solid acids were used for the first time as an electrolyte in a fuel cell ([6]). Leaving aside the solubility and the mechanical resistance, solid acids represent a valid alternative to other compounds, such as NAFION®. In fact, they do not need to be humidified, thus simplifying the design of the cell, and can operate at high temperatures of 200 ° C, increasing the CO tolerance. Moreover, they are impermeable to liquid hydrocarbons, making it possible to use them also for DMFCs. However, recent studies have shown that not all solid acids can be used in fuel cells. (Fig 2.3).

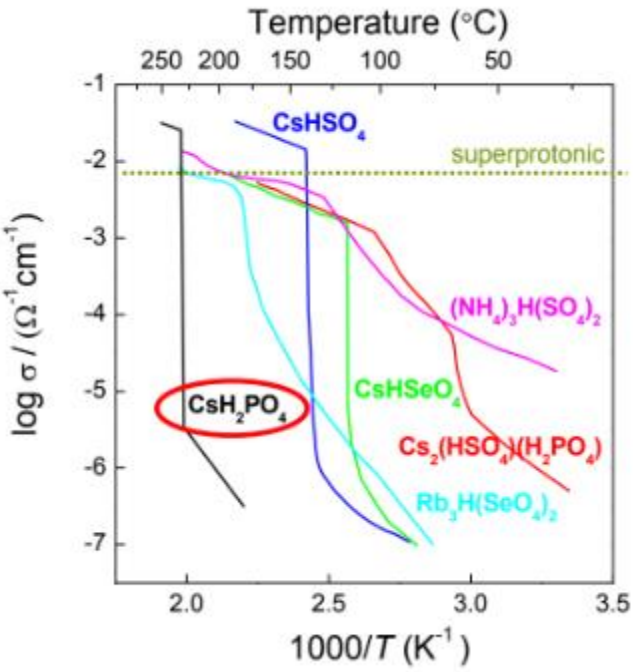

Fig 2.3- Proton conductivity of several solid acids

From Fig 2.3 it is easy to understand how the presence of sulfur and selenium affects the electrolyte stability. In fact, the sulfates and the selenates are not stable under hydrogen atmospheres and it is therefore preferable to use arsenates or phosphates, such as CsH_2PO_4 ([7])

2.2.1 REALIZATION OF ELECTROLYTE

We consider a based CsH_2PO_4 SAFCell (Fig. 2.4).

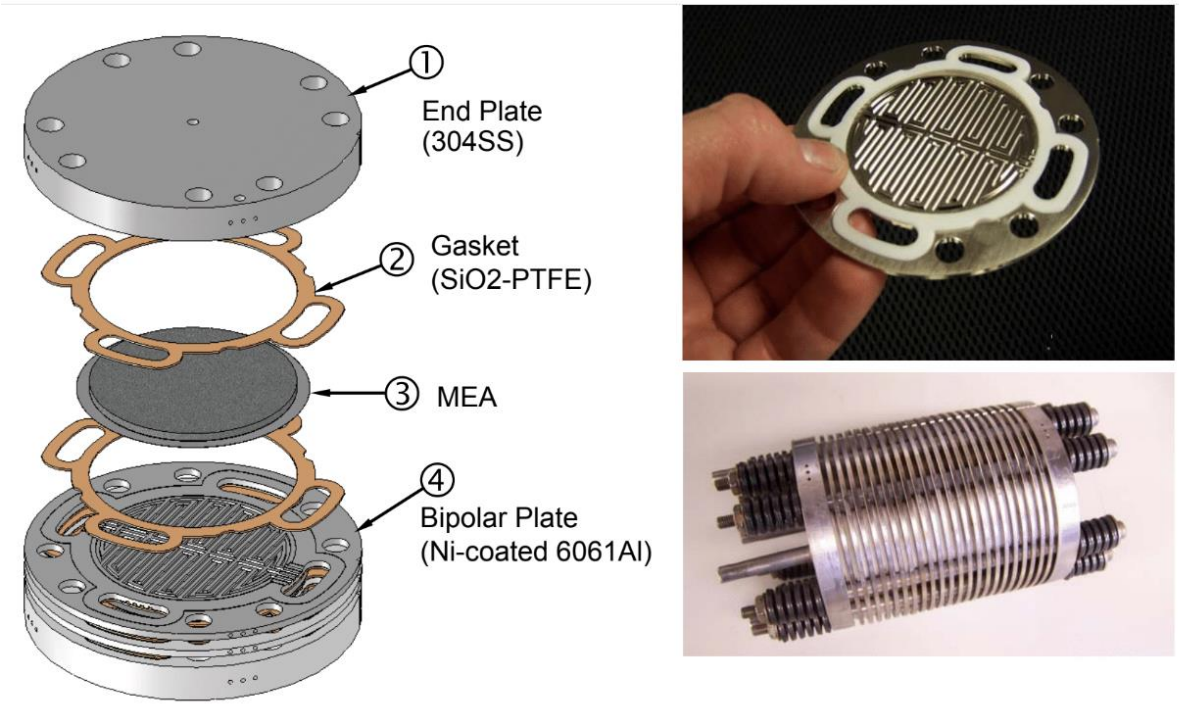

Fig 2.4- Stack design for a SAFCell and photo of a 20-cell stack

The electrolyte is synthesized starting from cesium carbonate atoms $CsCO_3$, 99.9% pure, dissolved directly in a methanol solution to which a stoichiometric amount of about 85% of phosphoric acid is then added H_3PO_4 ([8])

$$Cs_2CO_{3(CH3OH)} + H_3PO_4 \rightarrow CsH_2PO_4(s) + CO_2(g) + H_2O$$

The solid particles of CsH_2PO_4 they precipitate rapidly and their solubility in methanol is negligible. The precipitate is filtered and allowed to evaporate overnight at 80 ° C in a dry oven. Next, the material is dissolved again in a water / methanol mixture (34/66% by weight) and is then deposited on a carbon sheet by means of the

nano-spraydryer to form a thin film. The particulate distribution on the carbon substrate is determined using an electronic scanning microscope equipped with an EDX spectroscopy.

The stability of the CsH_2PO_4 as an electrolyte for fuel cell, it was demonstrated by Boysen and Otomo ([9]) ([10]). However, this compound, in conditions of insufficient humidity, loses stability (Fig. 2.5) and starts to decompose / dehydrate according to the reaction:

$$CsH_2PO_4\ (s) \rightarrow CsH_{2-2x}PO_{4-x}(s) + xH_2O(g)$$

$$0<x\leq 1$$

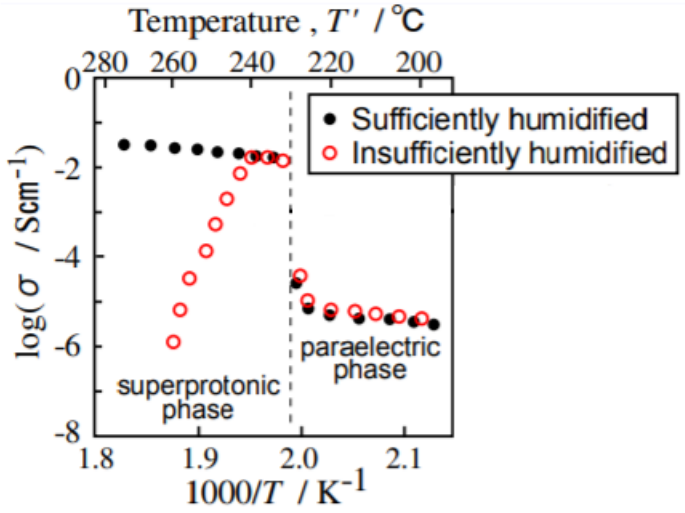

Fig 2.5- Decreasing of conductivity by dehydration

It is therefore important to see the progress of the compound during dehydration.

In this regard, a team led by prof. Taninouchi of the Kyoto University ([11]). The team also aimed to understand if the product of dehydration was a pyrophosphate $CsHPO_{3.5}$ (x=0.5) or a metaphosphate $CsPO_3$ (x=1). Laboratory experiments suggested that the effects observed on the conductivity were products of partial polymerization of the surface of the particles. X-ray analysis showed that the increase

in conductivity at 230 ° C coincided with the loss of mass caused by thermal effects. A range of temperatures between 230 and 260 ° C was considered. For the general dehydration reaction, the partial pressure of the water is given by

$$\log p_{H_2O} = 6.87(\pm 0.46) - 4.02(\pm 0.24) * \frac{1000}{T_{dehy}} \quad (2.1)$$

It is now necessary to understand the value of the actual temperature of dehydration. Consider the reactions

$2CsH_2PO_4$ (s) → $2CsHPO_{3.5}$(s)+ H_2O(g) (a)

CsH_2PO_4 (s) → $CsPO_3$(s)+ H_2O(g) (b)

To which they correspond

$$\ln p_{H_2O(1)} = -\frac{\Delta_{dehy}G_1}{RT} \quad (2.2)$$

$$\ln p_{H_2O(2)} = -\frac{\Delta_{dehy}G_2}{RT} \quad (2.3)$$

CsPO is more stable, and so it could be written

$2CsHPO_{3.5}$(s)→ $CsPO_3$(s)+ CsH_2PO_4 (s)

And so

$$\ln p_{H_2O(1)} - \ln p_{H_2O(2)} = -\left(\frac{\Delta_{dehy}G_1}{RT} - \frac{\Delta_{dehy}G_2}{RT}\right) = -\frac{\Delta_{dehy}G_3}{RT} < 0 \quad (2.4)$$

By (2.2) and (2.3) you could be obtain the temperature values

$$T^{(1)} = \frac{\Delta_{dehy}G_1}{R \ln p_{H_2O}} \quad (2.5)$$

$$T^{(2)} = \frac{\Delta_{dehy}G_2}{R \ln p_{H_2O}} \tag{2.6}$$

And so

$$\Delta_{dehy}G_1{}^{(T^{(1)})} - \Delta_{dehy}G_2{}^{(T^{(2)})} = -\left(T^{(2)} - T^{(1)}\right) * \Delta_{dehy}S_1 \tag{2.7}$$

We can write that

$$T^{(1)} - T^{(2)} = \frac{\Delta_{dehy}G_3}{R \ln p_{H_2O}} - \Delta_{dehy}S_1$$

where $\Delta_{dehy}S_1>0$ and $\ln p_{H_2O}<0$.

It's clear that $T^1>T^2$ and so the T_{dehy} is the temperature related to (b) reaction. This result from the thermodynamic point of view is also proceeding purely chemically. In the course of dehydration, in fact, there would be a change in weight of -7.84% to form $CsPO_3$ and a decrease of 3.92% to form the pyrophosphate. From the data collected, the researchers have seen that actually there is a weight loss of about 7%. Plotting the data we have also seen how the slope of the curve obtained (Fig 2.6) suggests that there are no intermediate compounds in the dehydration process

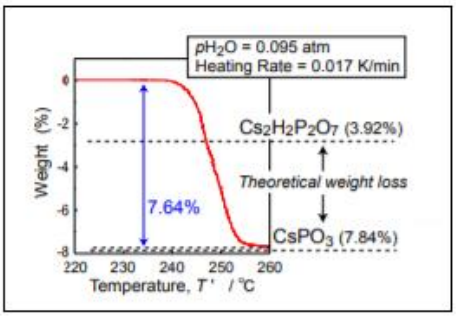

Fig 2.6- Thermalgravimetry under humidified condition

The collected data detected a transition structure at 238 ° C where the peak of the dehydration process is reached at a temperature of about 285 ° C.

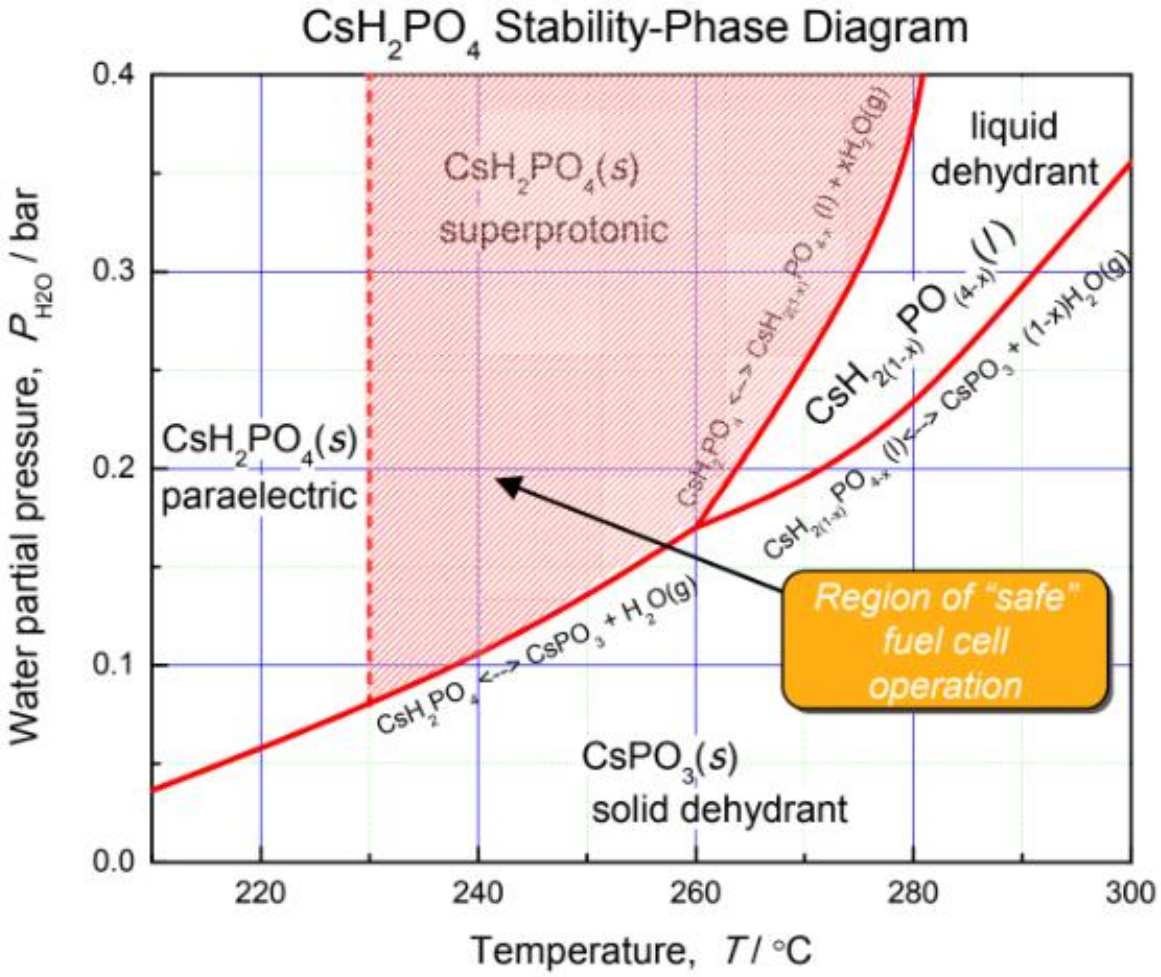

Fig 2.7- Stability-Phase diagram

From Fig 2.7 we see how with an equivalent pressure of P_{H2O} of 0.30 atm, the operating temperature of 270 ° C is sufficient to prevent dehydration

2.2.2 **EXPERIMENT** ([12])

To demonstrate how the use of moderate water pressure can guarantee the chemical stability of solid acid, a study on MEA has been carried out by Haile, Dane., Boysen & CO. ([13]). The MEA in question was made with an electrolyte formed by CsH_2PO_4 260 micron of thickness and a platinum electro-catalyst applied to both electrodes. The temperature of use was set at 235 ° C and the pressure P_{H2O} at 0.30 atm. After a stabilization phase of 24 hours, the experiment was carried out for 100 hours imposing a current density of 100 mA/cm^2. The results are shown in Fig. 2.8.

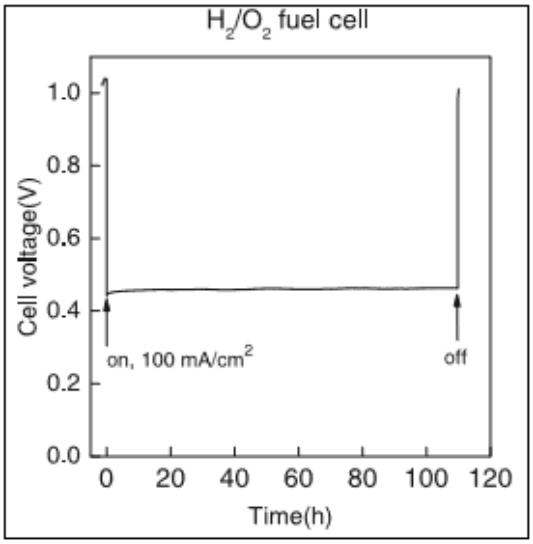

Fig 2.8- Cell voltage as a function of time on 100 mA cm^{-2}

As you can see, the tension remained fairly constant during the experiment, going from 0.441 V to 0.462 V with an average voltage that is around 0.460 V.

Subsequently, the trend of the current and voltage density before and after the 100h experiment was compared. the diagrams shown in Fig 2.9 could thus be traced.

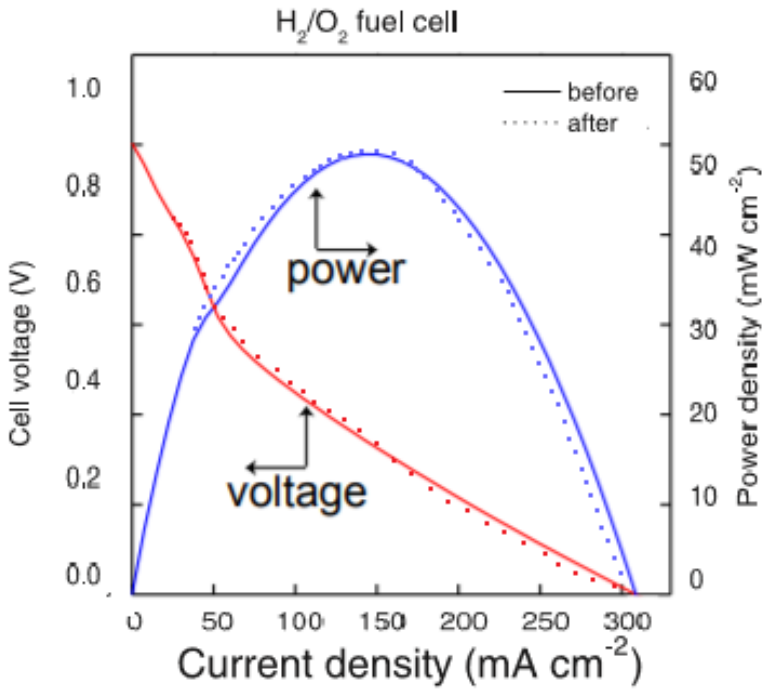

Fig 2.9- Cell voltage and power density before and after the measurement at 100 hours.

According to the Nernst equation, a theoretical OCV of 1.12 V should have been verified, but as we have seen, the value of 1.003 V for both measurements has been reached. This difference was attributed to fuel losses due to possible micro-fractures in the electrolyte. The maximum power is around 48.9 mW/cm^2 and the maximum current density around 301 mA/cm^2.

The experiment was then repeated substituting the previous MEA with another formed by Pt-Ru in order to use a DMFC (Fig 2.10)

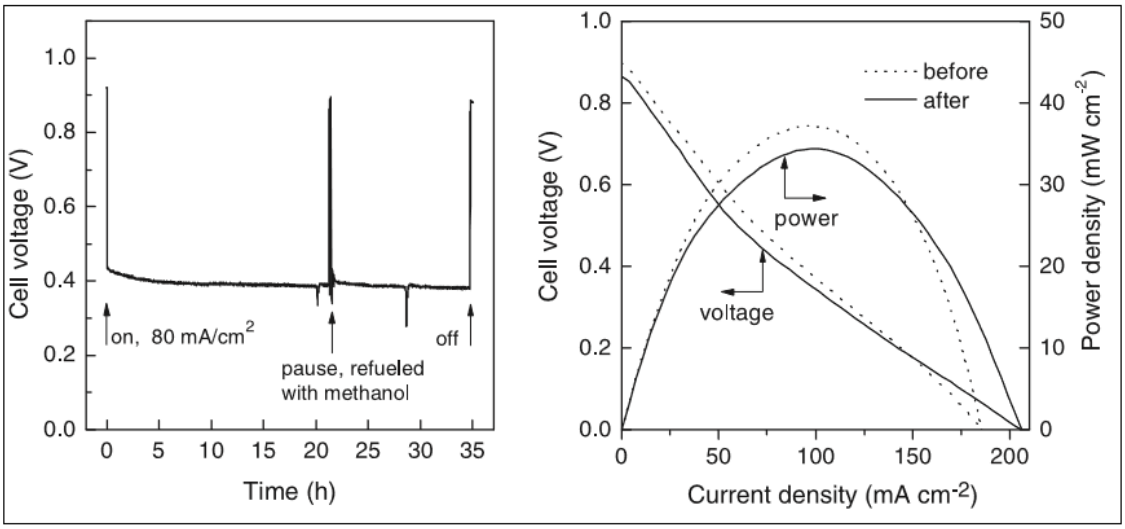

Fig 2.10- DMFC performance with the CsH_2PO_4 based electrolyte

. In this case the current density was 80 mA/cm^2 for 35 hours. The operating temperature was brought to 243 ° C. Also in this case it was possible to observe a certain constancy in the voltage reached with an initial value of 0.441 V and a final one of 0.381 V. The bias curves before and after the experiment are also quite similar, with a power peak of 37.2 mW in the first case and 34.4 mW in the second. The measured OCV was instead of 0.897 V before and 0.865 V after. Although these values are not comparable with those that theoretically should have been obtained, they are nevertheless higher than those of a polymeric electrolyte DMFC (0.8 V). This is due to the low permeability of the solid-acid membrane. About the stability of the superprotonic phase, both configurations are stable over time.

2.3 SAFCell: ADVANTAGES

A fuel cell with electrolyte formed by CsH_2PO_4, generally, operates at intermediate temperatures compared to those of the other fuel cells available on the market (Fig 2.11).

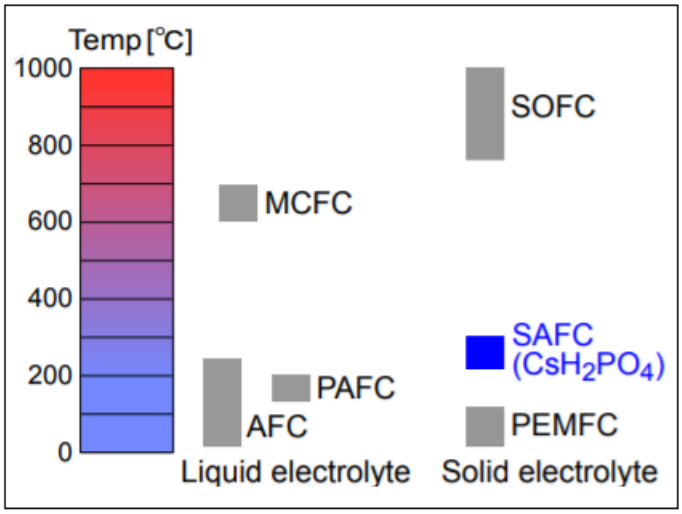

Fig 2.11- Range of temperature of different FC

. The temperatures reached, about 240 ° C, are suitable for increasing the electronic activity without having to face the drawbacks of other high temperature cells, such as SOFCs.

The operations in the fuel cells at quite high temperatures allowed by the solid acids allow to release the requirement of purity of the fuel. High impurity measures can be tolerated (>20% of CO, >250ppm of H_2S, >100ppm of NH_3, >1% NO) without affecting the performance of the cell. The use of pure hydrogen or reformed propane (see Tab 1) does not significantly affect the performance of the cell in terms of power obtained.

Tab 3- Reformed propane components

H_2	N_2	CO	CO_2	CH_4	C_3H_8	H_2S
41.1%	34.6%	10.6%	9.84%	0.24%	0.005%	0.5 ppm

The behavior of voltage and stack power is shown in Fig. 2.12 for hydrogen, a commercial propane reformate tested at staring and the same fuel after 4 hours. As you can see the behavior could be considered constant in time also using a fuel rich of several contaminants.

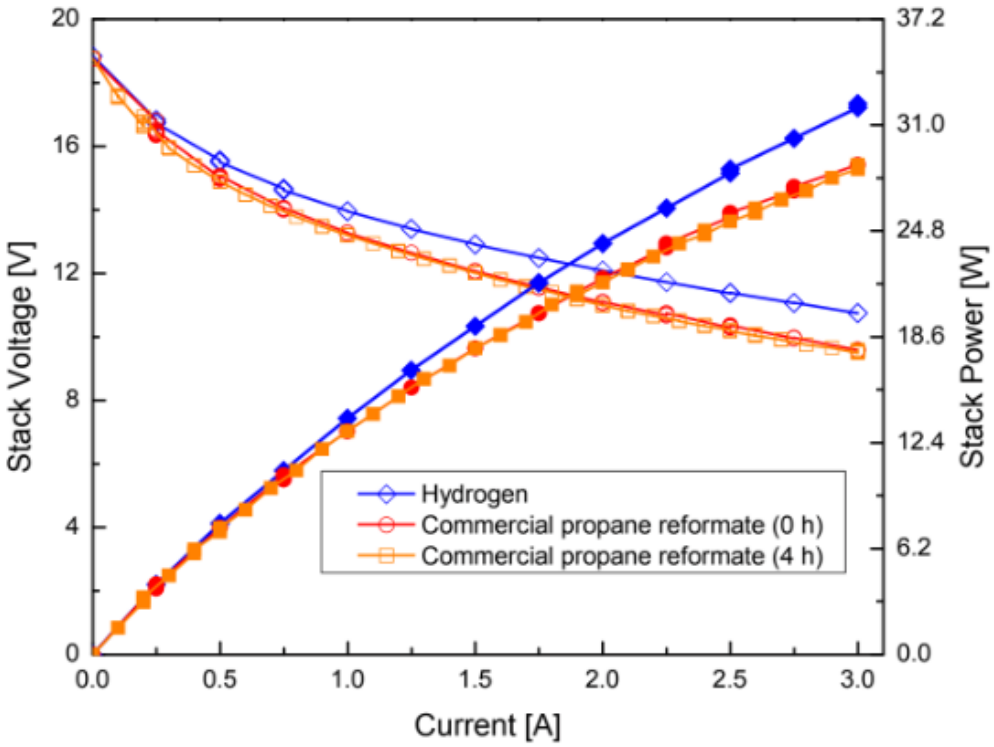

Fig 2.12- Performance of SAFCell using three different fuel

The high temperatures also make it possible to increase the catalytic activity and to have residual useful heat for cogeneration configurations, which are important for automotive applications. Solid acids allow the transport of anhydrous electrons and precautions such as removal of water from the cathode and charging to the anode are

not necessary. They are therefore suitable for Direct Methanol Fuel Cell (DMFC), where the nature of the electrolyte allows to increase the possibility of having membranes impermeable to methanol itself.

Although they are soluble in water, the operating temperatures above 100 ° C allow to have water in the form of steam, which is harmless to the otherwise soluble electrolyte.

Furthermore, the temperatures reached guarantee the functioning of the cell without the use of sought-after catalysts, as is the case for PEMFCs, thus reducing production costs (Fig. 2.13).

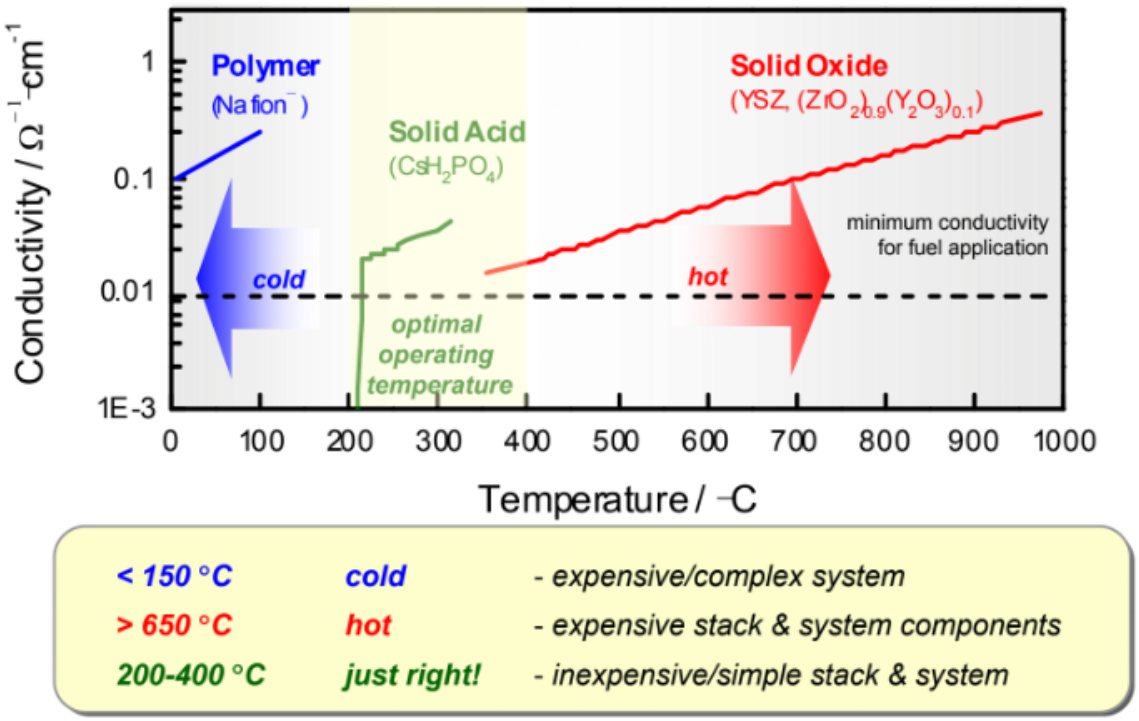

Fig 2.13- SAFCell advantages vs other FC as function of conductivity

2.4 SAFCell ON Sn TYPE VS SAFCell ON Cs TYPE

Recent studies have shown that SAFCell can also be used with the direct use of alcohols such as methanol. A research conducted by X.Chen and C. Wang of the University of Marylan ([14]) had the purpose of experimenting and testing various materials to obtain an electrolyte that would allow to maximize the yield of the plant working at temperatures in the order of 200 ° C. Among the various materials, the styosous phosphate of indium of formula has aroused deep curiosity $Sn_{0.9}In_{0.1}P_2O_7$. The researchers noted how this compound combined the advantages of SOFCs and PEMFCs, being able to conduct both ions O^{2-} and ions H^+ at temperatures between 130°C and 230°C.

The electrolyte was prepared by mixing the stannous oxide SnO_2, phosphoric acid H_3PO_4 and indium oxide In_2O_3. By bringing the components to 300 ° C, a very viscous dough is formed which is left to be calcined for about two and a half hours at a temperature of 650 ° C. After this process it is reduced to powder by a mortar and pressed to 250 MPa. The anode and the cathode are both formed by two layers: a diffusion layer and a catalyst layer. The diffusion layer is made up of 85% by weight of carbon and PTFE of 15% by weight. The catalyst layer is instead formed from 45% by weight of stannous phosphate of indium, 40% by PT / C and 15% by PTFE. The cell is then saturated with a mixture of methanol and water. The studies were carried out by comparing the conductivity of the $Sn_{0.9}In_{0.1}P_2O_7$ with CsH_2PO_4 one.

As shown in Fig.2.14 the conductivity of the $Sn_{0.9}In_{0.1}P_2O_7$ increases as the humidity of the cell increases. The maximum protonic conductivity is around 200 ° C with 40% of H_2O. It is equal to 0.019 $ohms^{-1}$ cm^{-1}, a value very similar to that achieved by CsH_2PO_4 (0.02) at 240°C.

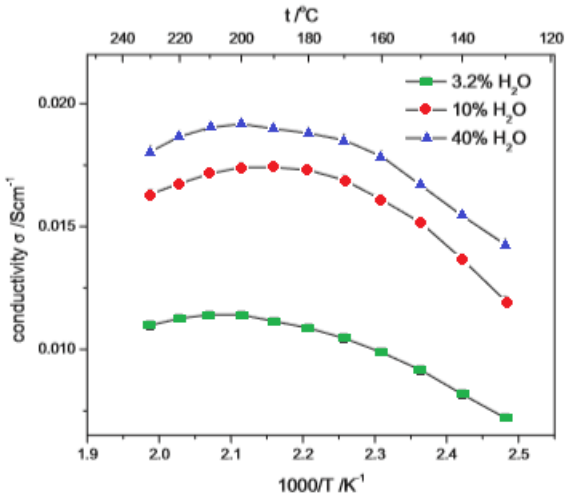

Fig 2.14- conductivity with various water vapour pressures

The reason why the conductivity decreases after 200 ° C is not yet clear, but is thought to be due to the leakage of water produced by the reaction

$H_2O(g) \rightarrow H_2 + ½\ O_2$

which would start at 260 ° C. The interactions between water vapor and oxygen vacations would be responsible for the proton conductivity of the $Sn_{0.9}In_{0.1}P_2O_7$. During operation, the ions H^+ generated at the anode they travel through the membrane towards the cathode to react with oxygen. We therefore have the reactions

Anode: $2CH_3OH + 2H_2O \rightarrow 12H^+ + 2CO_2 + 12e^-$

Cathode: $3O_2 + 12H^+ + 12e^- \rightarrow 6H_2O$

Total: $2CH_3OH+3O_2 \rightarrow 4H2O+2CO_2$

To verify the conductivity of the $Sn_{0.9}In_{0.1}P_2O_7$, the membrane impedance was measured in O_2-atmosphere and N_2-atmosphere, both in dry and wet condition. The results are shown in Fig 2.15.

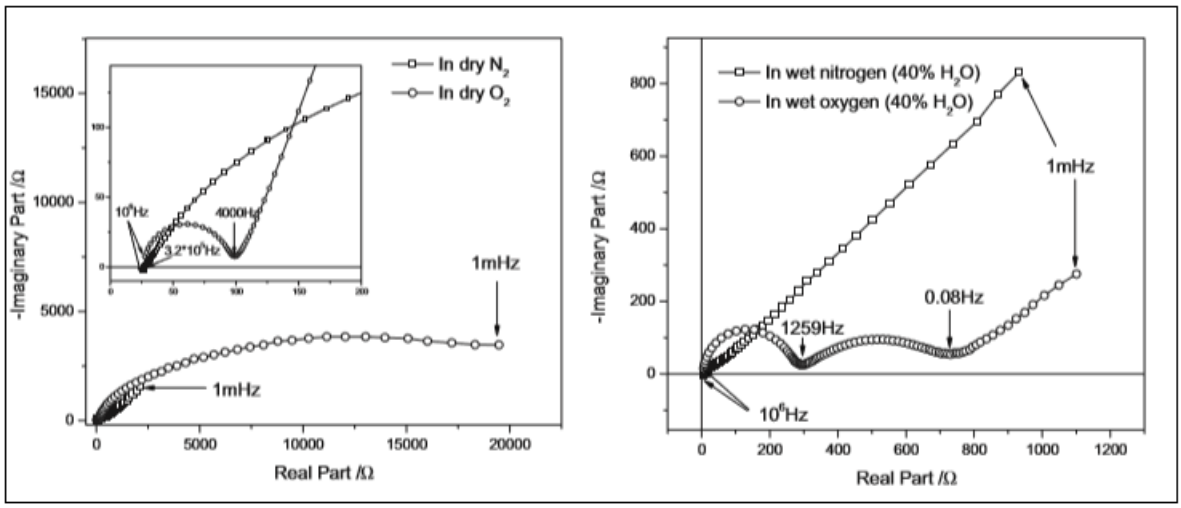

Fig 2.15- Impedance plots dry (left) and wet (right) condition at 170°C

As can be seen, the low-frequency line never intercepts the real axis, showing how the stannous phosphate of indium is an electrical insulator at a temperature of 200 ° C both in a dry and humid atmosphere. The experiment was then repeated by lowering the temperature up to 170 ° C for the $Sn_{0.9}In_{0.1}P_2O_7$ and at 235°C for CsH_2PO_4, in N_2-atmosphere with humidity of 40%. Both materials proved to be quite stable and therefore resulted in excellent electrolytes for fuel cells at intermediate temperatures. From (1.17) we obtain that the measured EMF is given by

$$E_0 = \frac{RT}{4F} * (t_{ion} * \ln\frac{p_{O_2}^P}{p_{O_2}^R} - 2t_{H^+} * \ln\frac{p_{H_2O}^P}{p_{H_2O}^R}) \quad (2.8)$$

where t_{ion} is the ion transport number, obtained from the sum of the proton transport number and the oxide ion transport number

.

$$t_{ion} = t_{H^+} + t_{O^{2-}} \quad (2.9)$$

Practise shows us that t_{H+} is bigger than t_{O2-} and so the equation (2.8) could be reduce to the formula

$$E_0 = \frac{RT}{2F} * (-t_{H^+} * \ln \frac{p_{H_2O}^P}{p_{H_2O}^R})$$

Because the theoretical EFM is given by

$$E_{Th} = \frac{RT}{2F} * \ln \frac{p_{H_2O}^P}{p_{H_2O}^R}$$

It's simple to evaluate t_{H^+} ing the formula

$$t_{H^+} = \frac{E_0}{E_{Th}} \quad (2.10)$$

In Fig 2.16 (left) the trend of this quantity has been plotted and it can be seen how it is in function of the temperature, with an average value of 0.76 in the range between 130 ° C and 180 ° C. In the same way we can calculate the t_{O2-}, whose results are shown when the temperature changes in fig 2.16 (right).

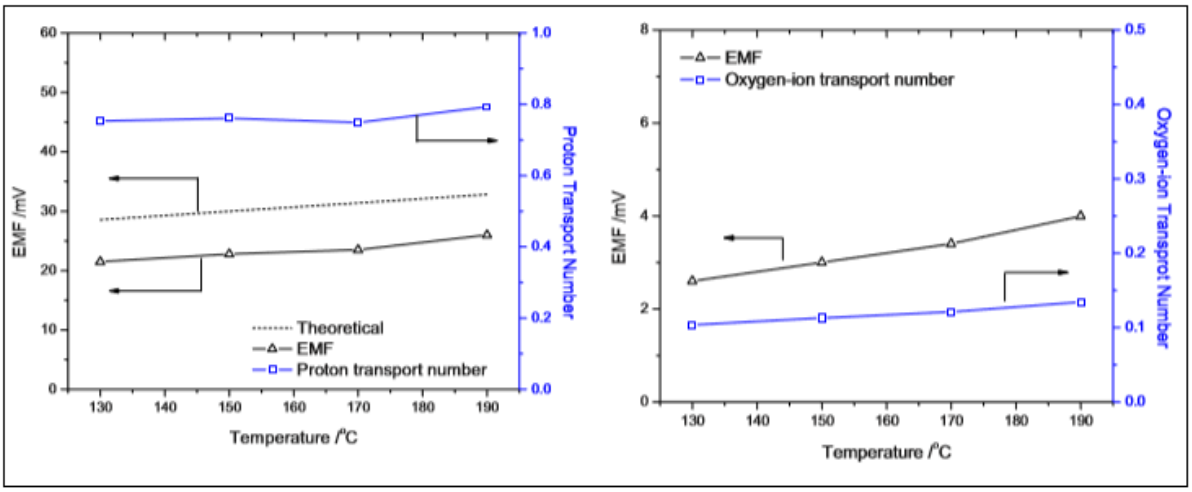

Fig 2.16-Proton (left) and oxygen-ion (right) transport number

The average value in this case stands at 0.12, so t_{ion}=0.88, a value lower than the unit attributed to the gas leak from the cell through the membrane.

Since the $Sn_{0.9}In_{0.1}P_2O_7$ allows the oxidation of carbon monoxide, its presence due to an incomplete reaction does not affect the system, unlike a system based on CsH_2PO_4. To confirm this, further experiments have been carried out by varying the percentage of CO in the fuel with a humidity of 40% at a temperature of 170 ° C in the case of $Sn_{0.9}In_{0.1}P_2O_7$ and comparing it with a proton conducting electrolyte (CsH_2PO_4) at 235 ° C. The experiment allowed to obtain the following results:

Tab 4- Results of the experiment for the CsH_2PO_4 and $Sn_{0.9}In_{0.1}P_2O_7$

	T [°C]	Power density $[mW/cm^2]$ 60%H2+40%H2O	Power density $[mW/cm^2]$ 45%H2+15%CH3OH+40%H2O	Power density $[mW/cm^2]$ 45%N2+15%CH3OH+40%H2O
CsH_2PO_4	235	17.3	13.7 (-21%)	2.1 (-85%)
$Sn_{0.9}In_{0.1}P_2O_7$	170	14.7	14.9 (+0.01%)	4.0 (-75%)

This behavior is attributed to the direct oxidation of CO to the anode by ions O^{2-} transported by the electrolyte membrane in stannous phosphate of indium. Thanks to

this phenomenon, together with the transport of H^+ ions that allow reactions (2.8) and (2.10), these cells can become the next generation of methanol cells

CHAPTER 3: MODELING

3.1 WHY SAFCell WITH METHANOL

The SAFCell represent as seen an excellent compromise between energy efficiency and economic savings. The low cost of the materials used and the temperatures of 300 ° C make it possible to make the most of the advantages of SOFC and PEMFC. But if on the one hand to exploit hydrogen to produce electricity it allows to obtain clean energy, on the other hand there is poor maneuverability and difficulty in transporting this energy carrier. To avoid these problems, you can think of using another fuel such as methanol.

Methanol is the simplest of alcohols and is also known as ethyl alcohol or wood spirit, since it was once obtained as a natural product of dry wood distillation. It is a flexible reactive compound which is liquid at room temperature (boiling point is 64.7 ° C) and has a density of about 790 kg/m^3 ([15]). It can be produced in an extremely simple way: just add an oxygen atom to the methane. Therefore, it can be obtained both from fossil fuels and from agricultural waste products and from the common urban waste. The first to talk about "methanol economy" as opposed to the emerging hydrogen economy was George Olah, Nobel Prize in Chemistry in 1994 ([16]). According to Olah, storing energy in the form of methanol, which is liquid, would have facilitated not only the storage, but also transport and use. A further advantage has always been suggested by Olah in the essay "The Methanol Economy", in which the Hungarian chemist explained how he had guessed that methanol could be obtained from water and carbon dioxide by means of electric power. By reforming carbon dioxide, Olah theorized that it could be possible to limit the effect of plants that burn natural gas or even directly capture the CO_2 present in the atmosphere in order to reduce the greenhouse effect. Further advantages are obtained if methanol and hydrogen are compared. There is greater efficiency in storing energy by volume, since the density of methanol is much greater than liquid hydrogen (71 grams / liter). This results in a higher concentration of hydrogen atoms in methanol (99 grams /

liter). Furthermore, the transport of methanol does not require a cryogenic container at very low temperatures and in the absence of a cooling system it does not evaporate. Nowadays there are two possible ways in which a Fuel Cell can exploit the methanol: through internal reforming it is possible to transform the methanol sent to the anode into carbon dioxide and hydrogen, or by directly reacting the methanol, as in the case of DMFC. In the following work the first case was considered, going to consider a SAFCell cell with electrolyte $Sn_{0.9}In_{0.1}P_2O_7$.

3.2 HOW TO CREATE AN ASPEN PLUS MODEL

The partial oxidation of methanol is an exotherm reaction indicated by the following reaction:

$$CH_3OH + 0.5\,O_2 \rightarrow CO_2 + 2H_2\ ,\ \Delta H^0_{298} = -155\ \frac{kJ}{mol}$$

The reforming reaction uses air and steam as feed reformer

$$CH_3OH + \left(\frac{S}{C}\right)H_2O + 0.5\left(\frac{O}{C}\right)O_2 + 0.5\left(\frac{O}{C}\right)\left(\frac{79}{21}\right)N_2$$
$$\rightarrow CO_2 + \left(3 - \frac{O}{C}\right)H_2 + \left(\frac{S}{C} + \frac{O}{C} - 1\right)H_2O + 0.5\left(\frac{O}{C}\right)\left(\frac{79}{21}\right)N_2$$

where S/C is the ratio between the vapor and the fuel carbon (methanol) and O/C is the ratio between the oxygen atoms in the oxidant and the carbon atoms in the fuel. Depending on these two reports, the content of H_2 in the reformed and its reaction enthalpy

$$x(H_2) = \frac{3 - \frac{O}{C}}{3 + \frac{S}{C} + 0.5\left(\frac{O}{C}\right)\left(\frac{79}{21}\right)}$$

$$\Delta H_{298}^{0} = \left(1 - \frac{O}{C}\right) \Delta H_R^T(STR) + \frac{O}{C} \Delta H_R^T(PO_x)$$

In general, current systems operate with an S / C between 1.3 and 2.0 and an O / C equal to 0.2. Numerous methanol processors have been studied and analysed over the years. The most famous is HotSpot fuel processor developed by Johnson Matthey ([17]). From the initial combustion the reactor is preheated and can thus produce hydrogen up to a power density of 3 kW / L. another methanol fuel processor was described by Ledjeff-Hey et al. ([18]). The system consisted of an evaporator, a steam reformer and a 7.5 mm thick separation membrane module. At 5 bars with an S / C of 2.0 a flow of hydrogen was generated equivalent to the power of 1.1 kW. The design for a methanol reformer suitable for use in a fuel cell was analysed by Zanfir et al. ([19])]. In his studies he noted that part of the reformed hydrogen leaves the unconverted anode. By reusing this hydrogen, it was possible to increase the overall efficiency of the cell. Based on the studies listed, it was decided to use an oxidative steam reforming operating with countercurrent heat exchangers. The layout of the chosen system is shown in Fig. 3.1

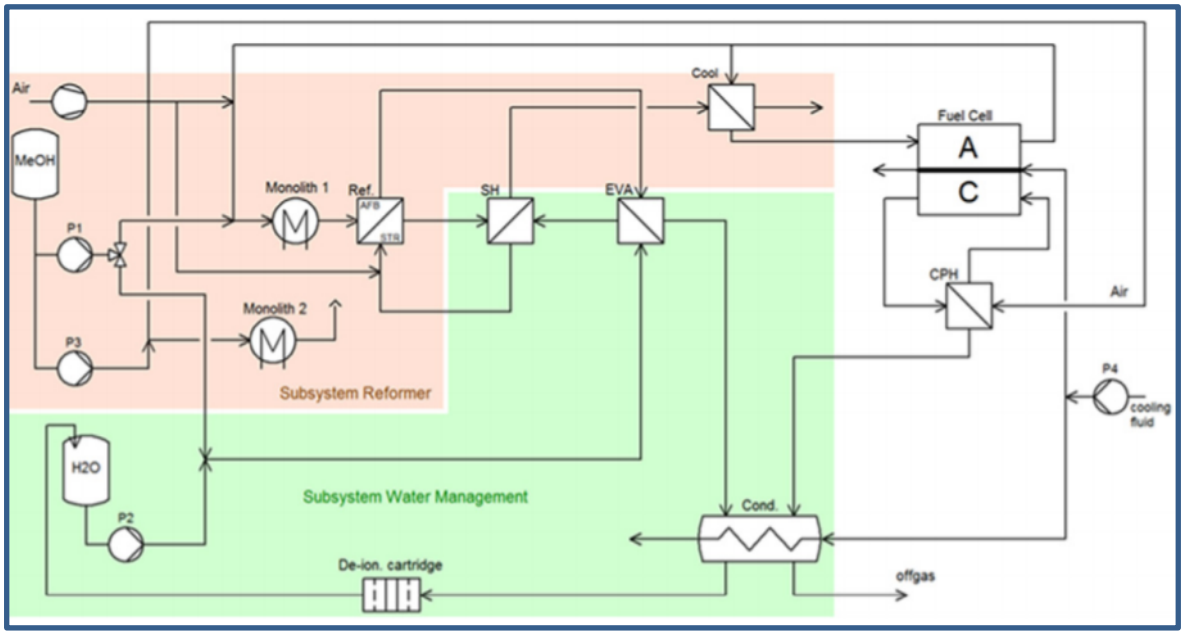

Fig 3.1- Layout of system

The system consists of three subsystems: a subsystem reformer, a subsystem water management and a subsystem power production. The subsystem reformer is formed by the reformer / afterburner pair (STR / AFB), which are responsible for transforming the methanol into hydrogen to be sent to the anode of the SAFCell. The methanol is mixed with water and subsequently evaporated in the evaporator (EVA) by heat exchange with the hot fumes coming from the burner and subsequently overheated by the hot reformed (REF1).

The subsystem water management is divided into two sections: one for the recovery of the heat produced by the cell and the burner, the other includes components that balance the gap between the thermal power recovered from the plant and that required by the user. This last section was not considered in the model, as the objective of the study is of another nature. Other systems that have not been modeled are those for collecting condensed water. For the latter attention was paid only that it was higher than the amount needed for the reaction in order to move forward.

The subsystem power production includes the SAFCell stack that produces direct current through the electrochemical reaction. Downstream of this stack there is a mixture of air and steam water as a product.

The selected SAFC stack is manufactured by SAFCell ®, Inc., with a stack of 64 cells, active area of 5 " (110 cm^2)(on the right in the Fig. 3.2), able to produce 1,4 kW ([20]).

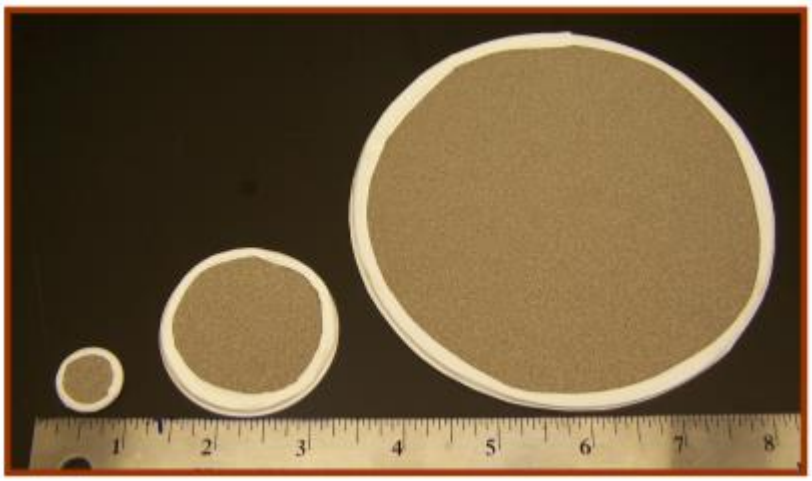

Fig 3.2- Three different MEAs:from left to right 3/4" D, 2" D, 5" D

As can be seen from the graph shown in Fig.3.3 at 200 mA/cm^2 with 64 cells corresponds precisely to a value of about 1400 W of electricity produced with a voltage of 0.8 V.

.

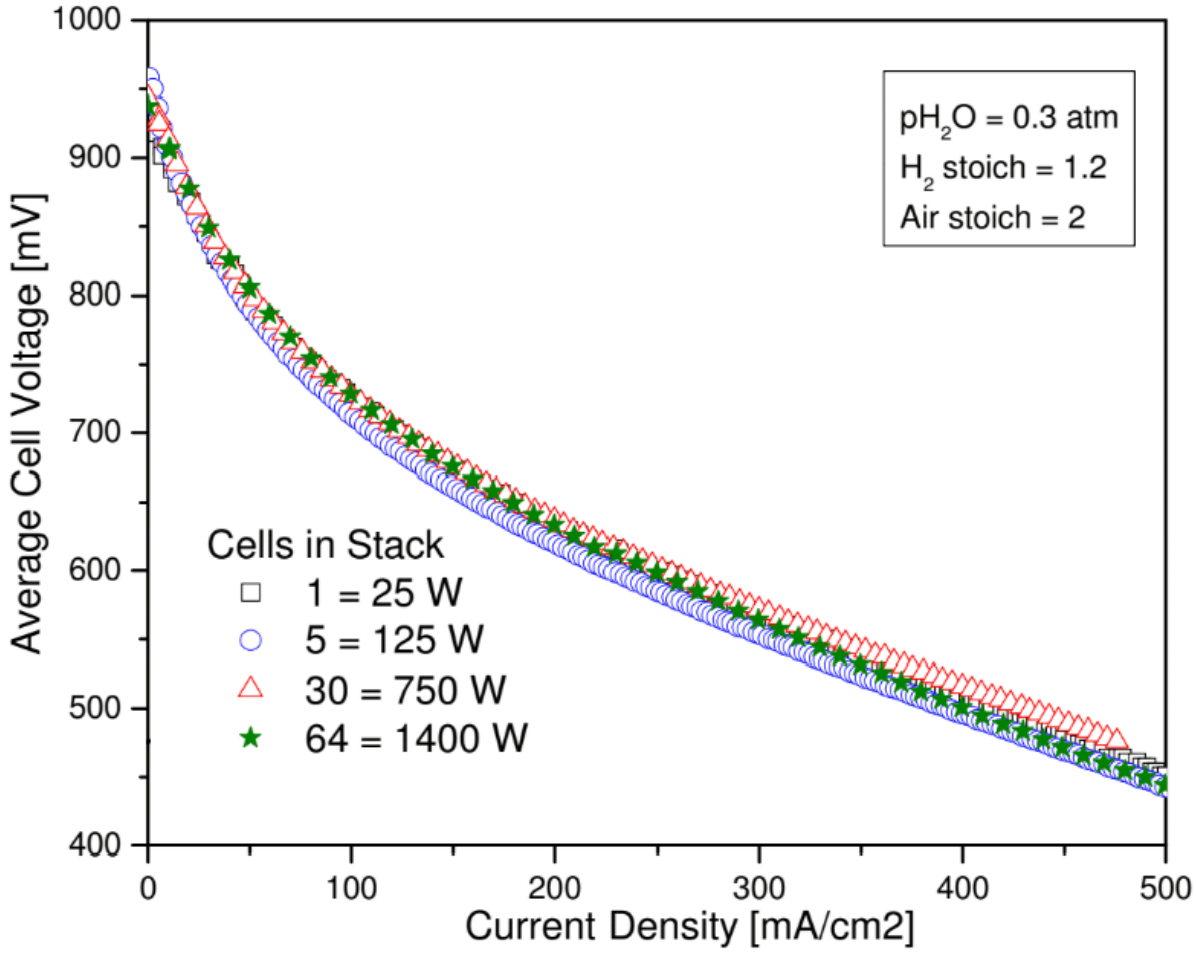

Fig 3.3- Average cell voltage for stack with different number of cell.

Below is a photograph of the SAFCell cell taken into consideration (Fig. 3.4).

Fig 3.4- 64 cell stack tested by Nordic Power Systems AS

When a fuel cell feeds a domestic user, or connects to the network, do not forget to transform the parameters of the electric current with a power conditioning. It consists of a DC / DC converter which raises the voltage from 20-60 V_{DC} to 400 V_{DC}, followed by a DC / AC inverter generating current at 230 V_{AC} and at frequency of 50Hz (if the plant is in Europe).

About the exchangers, cylindrical exchangers were considered with a series of pipes in parallel. In the inner tubes the cold flow has always flowed. In order not to complicate the discussion too much, some simplifications have been adopted. Pressure drops were not taken into account due to the low speeds and the velocity, pressure and temperature gradients were neglected in a radial direction, based on a plug-flow assumption. Finally, the surface of the pipe, the inlet section and the outlet section were considered well insulated. Since chemical reactions do not occur in the exchangers, the composition of the mixture passing through them is considered uniform.

The model has been implemented using the Aspen Plus software. This software works in two ways: in a single-domain and in a multi-domain approach, called sequential oriented mode. The software is powerful, because it allows to calculate the thermodynamic properties of pure components or mixtures, having available a large database of the various physical and chemical properties of various molecules. The simulation is zero-dimensional and each part is treated as a zero-space expansion box. For the implementation of a Fuel Cell on Aspen Plus, however, it is necessary to consider that the software is suitable for the simulation of chemical plants and therefore the FC must be implemented in the same way. The program does not know protons or electricity and the reactions are simulated by stoichiometric reactors and the flow of protons is represented by the flow of hydrogen. The flow scheme is shown in the scheme of the Fig. 3.5

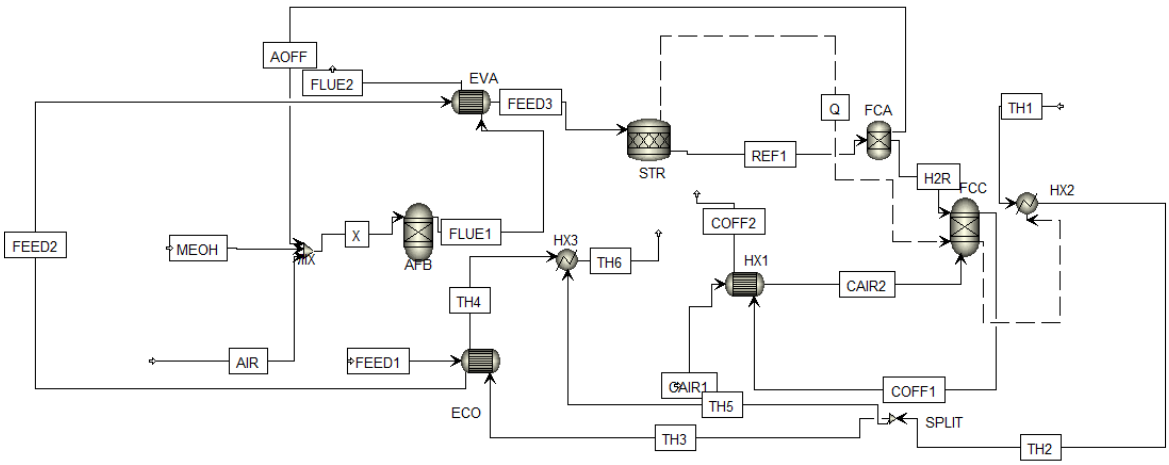

Fig 3.5- Flow scheme of the SAFCell system as implemented into ASPEN PLUS

The system consists of a feed evaporator (EVA), a reformer/burner (STR/AFB), a feed cooler (ECO), an air preheater to the cathode (HX1) and two heat exchangers for heat recovery (HX2 and HX3).

For the burner and the fuel cell cathode (FCC) the RGIBBS model used on Aspen was used, for the heat exchangers of the feed and air to the cathode the HEATX model was used, for the heat recovery exchangers it was the HEATER model was chosen, while for the reformer a RSTOIC reactor was used. The water methanol mixture (FEED3) is evaporated using the exhausted fumes coming from the burner AFB and then sent to the reactor. Here the reactions of SMR and WGS occur and the hot reforming (REF1) is sent to the anode. From here part of the fuel participates in the oxidation-reduction reaction going to generate the proton flow indicated with H2R, while part of the reformed (AOFF) containing water and carbon dioxide is re-introduced into the system to overheat the methanol and the air present before the burner. The flow of H2R and the air CAIR2, which was preheated in the exchanger HX1, to reach the operating temperature of the cell of 180 °C. The generated thermal power (QWASTE) is dissipated in HX2 via the TH1 flow. Even the exhausted fumes from the cathode are recovered by heat exchange and the water thus condensed is first deionized and then pumped into the tanks to be exploited in the WGS reaction.

3.3 PARAMETERS OF A SOFC AND A SAFCell

This paragraph lists the various parameters that have been appropriately chosen, based on the studies previously discussed in the discussion, to characterize a SAFCell and a SOFC to be able to compare them later with each other. In the characterization of the SAFCell the composition of the flows entering the system is considered constant. For simplicity, the flow of methanol formed only from CH_3OH, the flow of air formed by nitrogen and oxygen and that the water does not present salts dissolved inside it. The input flows are fed at pressure and at room temperature. The properties are summarized in Tab 3.

Tab 3- Inlet flux parameters

	Composition [*mol/mol*]		Temperature [*°C*]	Pression [*bar*]
Fuel	CH_3OH	1	20	1,013
Air	N_2 O_2	0,79 0,21	20	1,013
Water	H_2O	1	20	1,013

The list of chemical species has been reduced for simplicity to the reagents and products of the reactions of WGS and SMR: CH_3OH, N_2, O_2, H_2O, H_2, CO_2, CO. No carbon atoms formed during the various reactions were considered and negligible for the characteristics and temperatures reached by the cell the formation of NO_x.

The physical and chemical properties of the various fluids have been implemented based on the cubic state equation of Peng-Robinson, present in the Aspen Plus software.

As far as modeling is concerned, the major problem arises from having to take into account the reaction, heat exchange and hydrogen transport phenomena that take place through the Fuel Cell membrane. Therefore, the component's performance must be modeled considering both the polarization curve and the exchanges. thermals without giving up a zero-dimensional approach.

In the cell stack the power is regulated by varying the current. As the current of the caries changes, the rate at which hydrogen is consumed at the anode. In the cathode there will then be water formation due to a strongly exothermic reaction. It will therefore be necessary to consider the refrigerating fluid, in such a way as to be able to obtain the dissipation of the thermal power produced to maintain the temperature of the cell under acceptable operating conditions (200 ° C).

The polarization curve considered was taken from the studies conducted by the manufacturer SAFCell®, Inc. obtained for a stack of 50-cell and 50-cell methanol cells (Fig.). As already mentioned above, for this treatment a stack consisting of 64 cells was considered in order to obtain higher powers at the same intensity of current

produced, that is of fuel used.

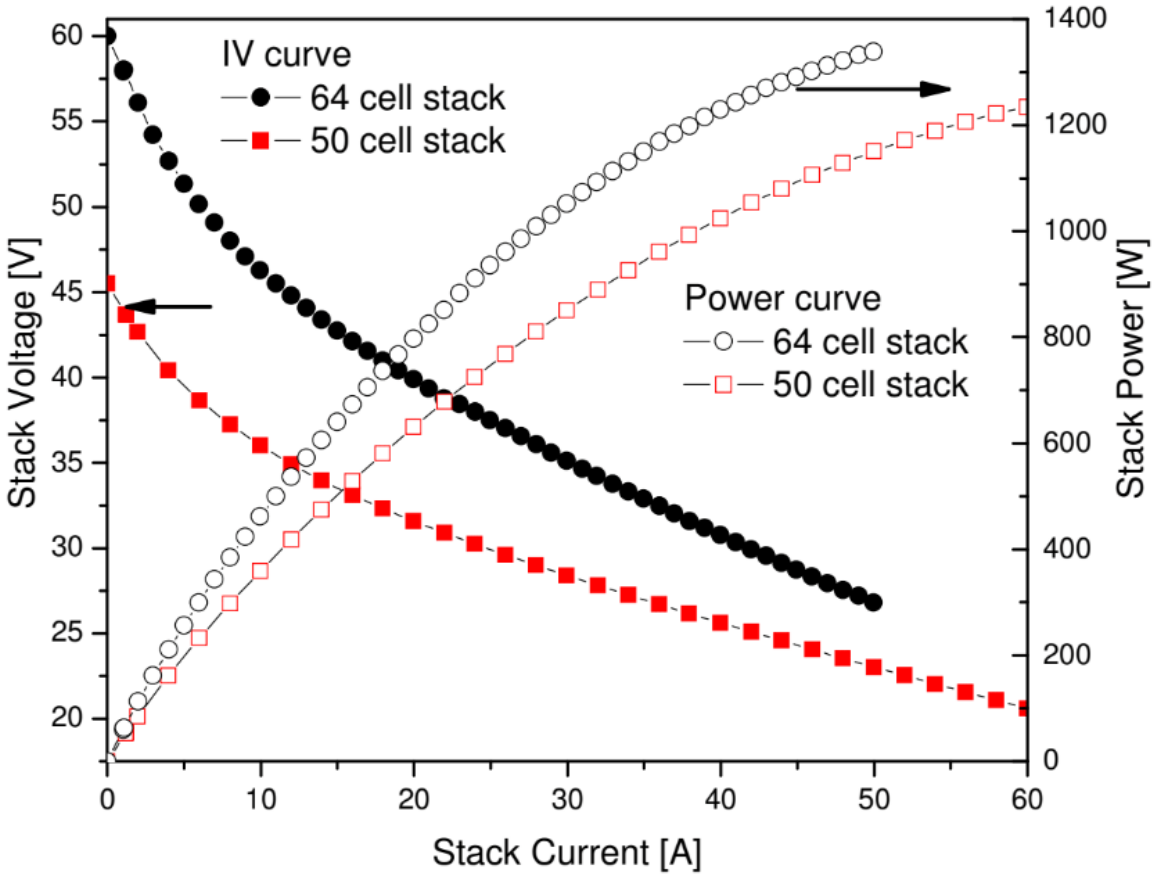

Fig 3.6- Comparisaton between 64 and 50 cell stack

The manufacturer data shows a current density of 0,238 A/cm^2, with an activation area of 110 cm^2 for a total current of 20 A. the electric power produced by the stack will therefore be:

$$P_{DC} = V * (i * A_{celle}) * N_{celle} \quad (3.1)$$

Considering this, to obtain the required power of 1.5 kW the number of cells and other data on the stack are shown in Tab.4.

Tab 4-Data of cell stack

P_{DC}	1500 W
N_{celle}	64
A_{utile}	110 cm^2
I	0,238 A/cm^2
I	22 A
V	0,897 V

The BURNER is controlled in such a way as to burn the mixture of the fluid X (exhausted gas, methanol and air) until it reaches a temperature of 300 °C in the FLUE1 (Fig 3.7).

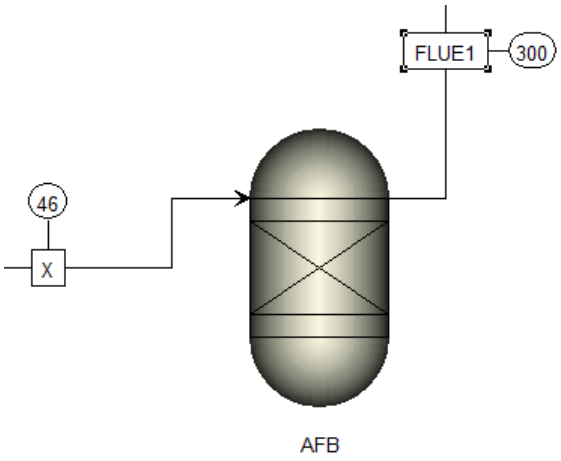

Fig 3.7- AFB inlet and outlet

FLUE1 is used as hot fluid in the EVA component, in which a mixture of methanol and water (FEED2) is preheated from a temperature of 20 °C till the temperature of 200 °C, before being sent to the reformer STR (Fig 3.8).

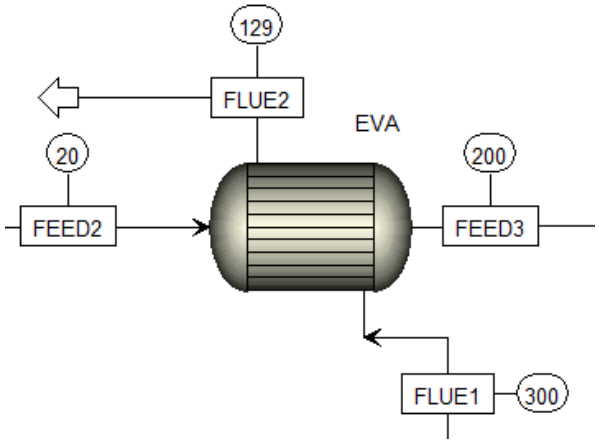

Fig 3.8- Inlet and outlet of EVA

Here the SMR occurs and there is formation of hydrogen and carbon dioxide starting from methanol and water. A thermal power Q is here generated and send to the cathode of the fuel cell to help the kinetics of the redox reaction (Fig. 3.9).

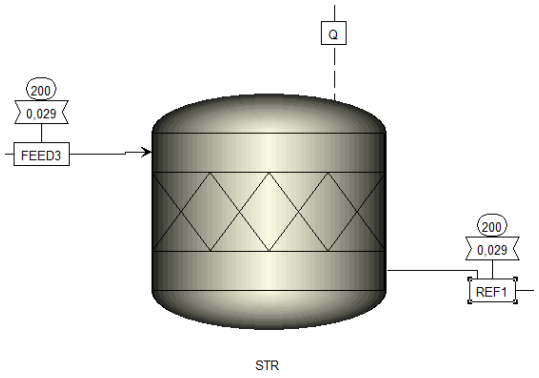

Fig 3.9- Inlet and outet flows and heat fluxs of hte STR

The REF1 reformate at a temperature of 200 ° C can thus enter the cell's anode. To simulate the flow of H^+ ions, a separator is then used, which imposes a flow of ions that allows to have an I = 22 A. The fraction H2R enters the cathode of the cell at a temperature of 200 ° C, together with a CAIR2 air flow at 160 ° C. The heat produced is then recovered in different ways: in part it is used to heat the air entering the cathode itself, which is in the CAIR1 ambient conditions. An additional fraction of QWASTE heat is recovered via a series of heat exchangers (Fig 3.10).

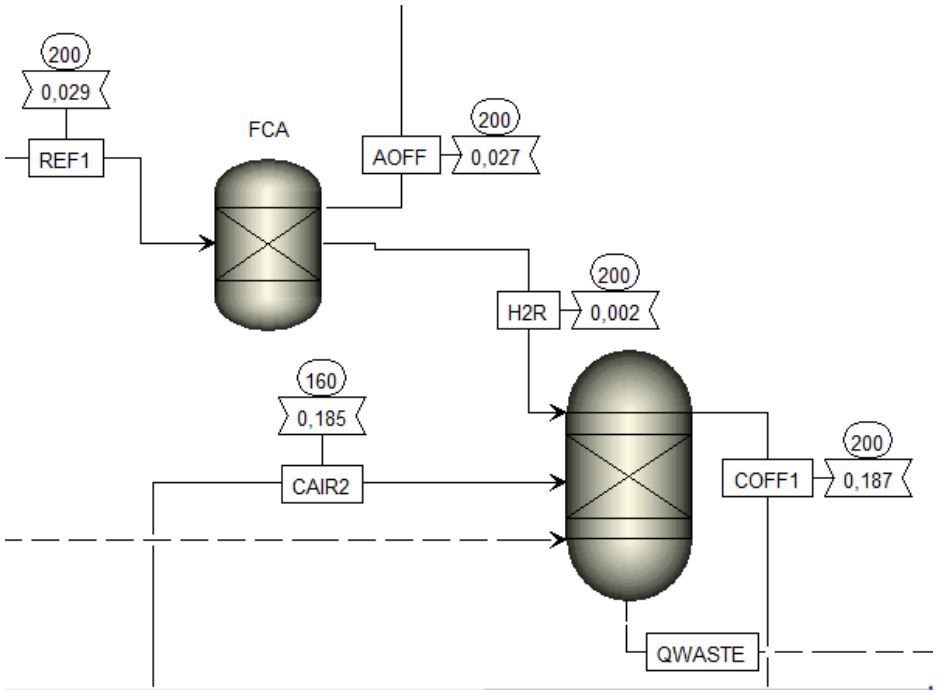

Fig 3.10- SAFCell stack : FCA (anode) and FCC (cathode)

For the modeling of SOFC, the following plant scheme was used instead (Fig. 3.11)

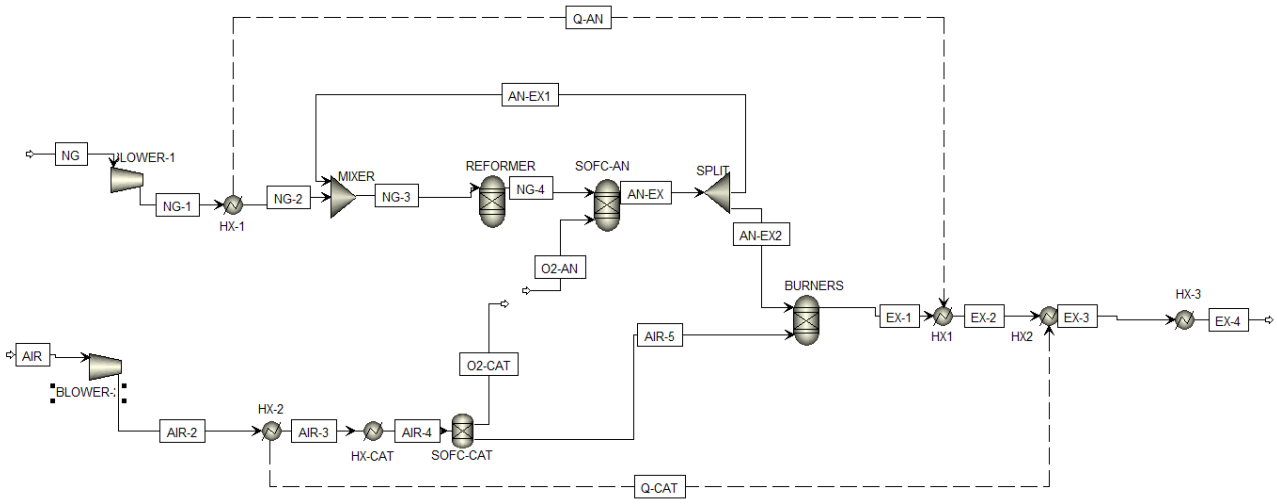

Fig 3.11- Flow scheme of the SOFC system as implemented into ASPEN PLUS

For the highest temperatures reached in this type of system, heat exchangers were increased in order to recover as much heat power as possible. As fuel, NG natural gas was chosen, assuming that it was made up exclusively of methane CH_4. As in the case of the SAFCell the temperature and the pressure are considered the ambient ones (see Tab 5). In the plant, therefore, a BLOWER is inserted both on the cathode side and on the anode side to bring the pressure to the operating value of 1.2 bar. Water is not required in this case.

Tab 5- Inlet flux parameters

	Composition [*mol/mol*]		**Temperature** [*°C*]	**Pression** [*bar*]
Fuel	CH_4	1	20	1,013
Air	N_2	0,79	20	1,013
	O_2	0,21		

CHAPTER 4: CASE STUDY

4.1 MOUNTAIN CABIN

The scenario considered for the operation of the fuel cell is that of a cabin. The problem of supplying electricity to isolated homes is of great current importance. From the website of the major distribution companies it is easy to check how the price of the connection operation is calculated in relation to the type of supply of the distribution company, adding the "Distance share", "Power share" and "Fixed share" contributions. For “Distance share”, the distance in a straight line from the nearest transformer station in service has been calculated for at least 5 years. As the distance increases, the costs obviously increase. Up to 200 meters there is a fixed cost of € 185 to which the following shares are added ([21])

- From 200 to 700 m € 93 for every 100 meters;
- From 700 to 1200 m € 185 for every 100 meters;
- Over 1200 m 369 € for every 100 meters.

In the case of isolated shelters typical of the Alpine landscape, the costs for the transport of electricity are added to the connection costs. It is therefore not difficult to grasp figures that stand at hundreds of thousands of euros. For this reason, the use of fuel cells for family consumption can represent a valid alternative not only from an environmental point of view, but above all economic.

4.2 DAILY LOAD

For this analysis we chose to size the system in such a way that all the electricity demand can be satisfied by the fuel cell stack. In this sense, therefore, we want to make each individual stable independent of the electricity grid, cancelling the costs of connection to

the national electricity grid. Typically, the average household consumption does not exceed 3 kW, but since here we are talking about alpine refuges, a reduction in electricity needs of around 30% was assumed. In the model considered, the stack was then appropriately scaled to obtain a power of 2 kW in DC.

For the purposes of the discussion, the electricity consumption data for some huts of the Bedole Refuge were considered ([22])

The Bedole Refuge is an outpost refuge for high altitude mountaineering. Located in Val Genova (TN) consists of a series of rooms for individual overnight stays and common areas represented by kitchens and bathrooms (Fig. 4.1).

Fig 4.1- Bedole Refuge

Inside it there are a series of electric commands that are described in detail in the Tab 6.

Tab 6- Load of the Bedole Refuge

N°	LOAD
30	Led lamps night departments
6	Led lamps bar/kitchen
1	Fridge
2	Freezer
1	Dishwasher
1	Washing machine

The performance of the plant was considered in two different periods of the year:

• summer in which consumption is on average less, attributable to a lack of use of air conditioners and a reduction in electricity consumption as the hours of light are greater than those of darkness;

• winter: where consumption is more focused on meal times and evening hours.

The results are shown in Fig 4.2.

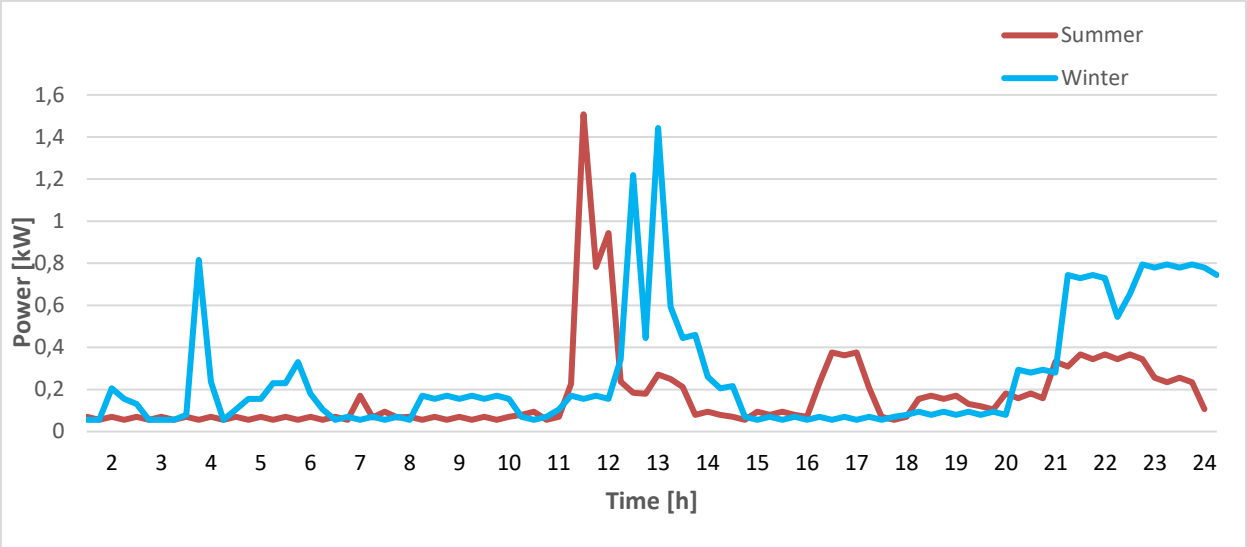

Fig 4.2- Daily load for a chalet in summer (red line) and in winter (blue line)
As you can see, consumption peaks refer to the periods when the shelter's kitchen works.

For both periods it is seen how the use of 2 kW producing stacks is more than sufficient even in the case of an electric power request that would exceed the maximum value considered (1.58 kW).

4.3 RESULTS

Two factors have been taken into account in order to make a comparison between the two technologies analyzed and modeled on ASPEN PLUS. The first is that both cells are asked to work continuously for 24 hours to produce a power of 1500 W. This value comes out from the analysis of the consumption loads of the Bedole Refuge. As for the surplus that would create an excellent solution could be the use of an accumulation system. In this way the cell would reduce its operating period. It was initially assumed to use the surplus in the winter months to satisfy the building's thermal use, but no idea came up for its use in the summer season.

To estimate the storage capacity, it is considered the balance of energy expresses by the formula:

$$N_{day} * \sigma_{load} = U_{nom} * C_{nom} * DOD \quad (4.1)$$

In which N_{day} is the number of utilization of charging battery (in this case it is supposed equal to 2), σ_{load} is the daily load (refer to the consumption of Fig. 4.2), DOD is the factor utilization (80% if we used a lithium battery). Whit these data the capacity of battery is around 10 kWh. To satisfy the requirements, it was decided to use a Tesla Powerwall 2 type of battery ([25]). The Tesla Powerwall 2 battery capacity has been increased from 6.5 to 13.5 kWh compared to the first model and is equipped with an inverter. This can be a solution in many countries, such as California, where electricity is very expensive. It boasts a power of 7kW peak and 5kW continuous, and an efficiency of 90%, with a depth of discharge of 100%. The operating temperature ranges from -20 ° C to 50 ° C and has an important weight of 122 kg. The available model is represented by a single size 13.5 kWh and its technical specifications are shown in Tab 7.

Tab 7- Technical specification of Tesla Power 2 battery

Dimensions (HxLxP)	115 x 75 x 15 cm
Capacity	14 kWh
Power	7 kW(pick) / 5 kW (continously)
Efficiency	90 %
Working temperature	From -20°C to 50°C
Weight	122 kg

The units are stackable, precisely because they are born with the concept of being combined according to the real needs of consumers. The efficiency is quoted around 90% for the AC current and 89% for the DC current. The Tesla 2 Powerwall has an integrated cooling system, which guarantees excellent functionality and a declared temperature between -20 ° C and 50 ° C. As far as noise is concerned, it is around 50 dB. The battery can be perfectly integrated with the photovoltaic system that you have already installed in home, but for this work it is

suppose that it is related at a Fuel Cell. The cost of this battery is around 6,400 and, however, must be added to the support equipment that costs another € 580 and the installation costs from € 950 to € 2,300. The plant is shown in Fig 4.3

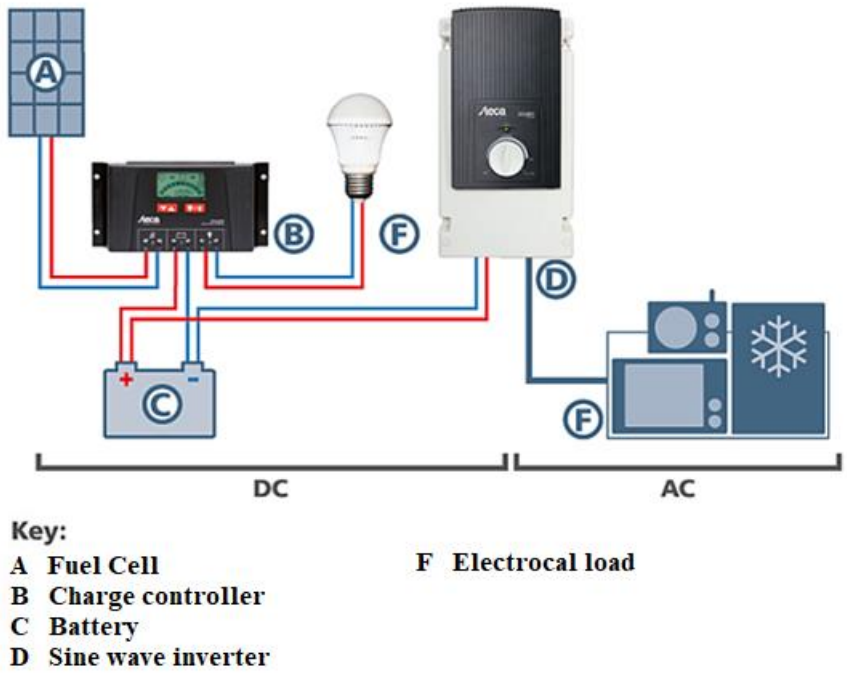

Fig 4.3- Storage system

As an inverter we chose instead to use Steca Solarix PI. Inverter systems are designed as solar home systems. The central solar charge controller ensures the battery is charged correctly and protects it against overcharging. In addition, a stand-alone inverter is connected directly to the battery in these systems so that AC appliances can be operated. If DC appliances are also used, they can be connected directly to the charge controller. An AC system can be created with a system voltage or battery voltage of 12 V, and also with 24 V or 48 V for greater capacities.

In this discussion the formula (4.1) was considered in order to calculate the actual daily consumption cost of the cell.

$$C = G_{fuel} * P_{fuel} * 24 \qquad (4.2)$$

Where G_{fuel} is the fuel flow in kg/h, P_{fuel} is its price in euros/h and 24 represents continuous operation throughout the day.

In order to be able to make an effective comparison, it was therefore necessary to calculate first the consumption required by the two solutions in order to obtain the prefixed power. The ASPEN PLUS software was very helpful in this. In the case of SOFC this value is equal to the consumption of the NG flow, the only fuel to power the plant. The simulation showed that its value is around 0.16 kg/h. With continuous use during the 24 hours we would therefore consume 3.81 kg of CH_4. As reported by the major supply companies ([23]) its price is currently around 0.98 euros/kg. There is therefore a total expense of € 15.25.

As for the SAFCell it must be considered that the fuel used is present in two flows: MEOH and FEED1. While in the first fluid its composition is totally CH_3OH, in the case of FEED1 the methanol / water ratio is fixed 2/3. The methanol consumed is then calculated using the formula (4.2)

$$G_{CH_3OH} = MEOH + 0{,}4 * FEED1 \tag{4.3}$$

In this way the value of G_{CH3OH} =0,528 kg/h.

Here we used the values reported by the national suppliers ([24]) too and the value found is 1.2 euro / liter.

From (4.1) we obtain a value of 14.50 euros. Schematic resume is shown in Tab 8.

Tab 8- Flow cost for both technologies

Cell	Fuel	Mass flow [*kg/h*]	Price [*euro/kg*]	Cost [*euro/day*]
SOFC	CH_4	3,81	0,98	15,25
SAFCell	CH_3OH	0,528	1,2	14,50

Depending on the type of the component, the Bare Erected Cost (BEC) can be calculated. All the data for the purchased cost of the equipment and the following relations have been taken by the Turton ([26]).

The BEC is calculated in two different ways_

$$C_{BEC} = C_p^0 * F_{BEC} \tag{4.4}$$

$$C_{BEC} = C_p^0 * (B_1 + B_2 * F_M) \tag{4.5}$$

The (4.5) is used for Heat Exchangers, the (4.4) in all other cases. In the formulas:

- F_{BEC} is the bare erected module cost factor accounting for specific materials of construction depending on the operative temperature and pressure conditions;
- B_1 and B_2 are constant parameters given in the tables;
- F_M is the material factor, which depends on the operative temperature;
- C_P^0 is the purchase cost of equipment referred to the bas conditions and can be expressed as:
-

$$C_p^0 = K_1 + K_2 * \log_{10} A + K_3 * (\log_{10} A)^2 \tag{4.6}$$

In which K_1, K_2 and K_3 are constants to fit the expression to the real costs of the device and A is the capacity of size parameter for the specific equipment. This equation is valid for a certain range of values of A. if operating conditions are not included in the range, C_P^0 will be calculated for the lowest value of A using the scale factor:

$$\frac{C_p^1}{C_p^0} = (\frac{A_1}{A_0})^n \tag{4.7}$$

Where n is the cost exponent and it is a parameter of the component depending on the class of equipment being represented. In the absence of other information, the coefficient n is taken as 0.6 and it comes from the six-tenths-rule. Since the purchase cost is referred to a specific year, it has been used the following expression to refer C_P^0 to another year using the time factor:

$$\frac{C_1}{C_2} = \frac{I_1}{I_2} \tag{4.8}$$

I is the cost index and in this work it is used CEPCI. The C_P^0 is referred to 2001 in Turton, so in order to reach the value for 2017 the CEPCI is assumed as 394 for 2001 and as 567,5 for the 2017. Both for SOFC and SAFCell the method is used to investigate the cost of all components.

4.3.1 SOFC cost analysis

For compressor the parameter A is the fluid power. The two compressor BLOW1 and BLOW2 absorb a nominal electric power respectively of 2 W and 19 W. these values are not included in the range value of the A and so it is used the equation (4.7). basing on the maximum temperature on the data it has been assumed two axial compressors, meanwhile in the typical operating range (<350°C) Carbon Steel (CS) has been assumed. The values are collected in Tab.9.

Tab.9 - Parameters and C_{BEC} for compressors

Component	K_1	K_2	$-K_3$	*A[kW]*	A_{min}	A_{max}	C_p^0	*n*	C_p^1	F_{BEC}	$C_{BEC}2001$	$C_{BEC}2017$
BLOW1	2,2897	1,3605	0,1027	0,002	450	3000	150027	0,6	92,22	3,9	359,68	249,72
BLOW2	2,2897	1,3605	.0,1027	0,19	450	3000	150027	0,6	1417,41	3,9	552,79	383,78

The REFORMER and the BURNERS can be described as a vertical pressurized vessel. In order to calculate the C_P^0 it is necessary to calculate the volume of the vessel that is the parameter A. The equation to calculate the volume is:

$$V_{vessel} = G_{v,m} * \tau \quad (4.9)$$

Where $G_{v,m}$ is the average volumetric flow rate between inlet and outlet streams of the burners and τ is the gas residence time in the burner (assumed 0.5 seconds).
The F_M is chosen considering the high temperatures and a Stainless Steel (SS) material.
The values are collected in Tab 10.

Tab.10 - Parameters and C_{BEC} for burner

Component	K_1	K_2	K_3	$A[m^3]$	A_{min}	A_{max}	C_p^0	*n*	C_p^1	F_{BEC}	$C_{BEC}2001$	$C_{BEC}2017$
REFORMER	3,5565	0,3776	0,0905	4,93e-4	0,1	628	1859,52	0,6	76,69	1,49	230,85	160,28
BURNERS	3,5565	0,3776	.0,0905	0,012	0,1	628	1859,51	0,6	521,09	1,49	1568,47	1088,95

In order to calculate the C_p^0 of the Heat Exchangers, it is necessary to calculate their area, i.e. the parameter A. the equation of heat exchange is:

$$Q = A * U * \Delta T \quad (4.10)$$

Where Q is the exchanged heat power [W], U [$W/(m^2K)$] is gas-to-gas global heat transfer coefficient (assumed equal to 100). By ASPEN the different Q are obtained and as material the CS has been chosen. The values are collected in Tab.11.

Tab.11 - Parameters and C_{BEC} for Heat Exchangers

Component	K_1	K_2	$-K_3$	$A[kW]$	A_{min}	A_{max}	C_p^0	*n*	C_p^1	B_1	B_2	$C_{BEC}2001$	$C_{BEC}2017$
HX1	4,1884	-0,250	0,1974	2,8e-3	10	1000	13661,5	0,6	101,4	0,96	1,2	220,03	152,76
HX2	4,1884	-0,250	0,1974	0,17	10	1000	13661,5	0,6	1193,8	0,96	1,2	2590,55	1798,55
HX3	4,1884	-0,250	0,1974	0,07	10	1000	13661,5	0,6	702,9	0,96	1,2	1525,28	1058,96
HX-CAT	4,1884	-0,250	0,1974	0,019	10	1000	13661,5	0,6	325,5	0,96	1,2	706,35	490,40

Starting from the obtained results, it is possible calculate the TASC of every component, taking into account the methodology provided by NETL ([27]). (Tab 12).

Tab 12- Capital cost level

Parameters	*Range from NETL report*	*Description*
Engineering, Procurement, Construction Cost (EPCC)	8%	% of BEC
Total Plant Cost (TPC)	30%	% of EPCC
Total Overnight Cost (TOC)	20.2%	% of TPC
Total As-Spent Cost (TASC)	11.4%	% of TOC

The results are shown in Tab 13

Tab 13- From CBEC to TASC

Component	C_{BEC} *2017*	*EPCC*	*TPC*	*TOC*	*TASC*
BLOW1	249,72	269,70	350,61	421,43	469,47
BLOW2	383,78	414,49	538,84	647,68	721,52
REFORMER	160,28	173,10	225,03	270,48	301,32
BURNERS	1088,95	1176,06	1528,88	1837,72	2047,21
HX1	152,76	164,99	214,49	257,81	287,20
HX2	1798,55	1942,43	2525,18	3035,25	3381,27
HX3	1058,96	1143,68	1486,79	1787,11	1990,854
HX-CAT	490,40	529,64	688,53	827,61	921,96

Summing up the values of the TASC and a SOFC (4295 euros), we get a total cost of the plant of 16060 euros.

4.3.2- SAFCell cost analysis

Applying the same methodology for SAFCell we are able to evaluate the cost of the plant. The summarized results are shown in Tab.14.

Tab.14 - Parameters and C_{BEC} for SAFCell

Component	K_1	K_2	K_3	$A[m^3]$	A_{min}	A_{max}	C_p^0	n	C_p^1	F_{BEC}	$C_{BEC}2001$	$C_{BEC}2017$
AFB	3,5565	0,3776	0,0905	4,13e-4	0,1	628	1859,52	0,6	69,09	1,49	207,98	144,39
STR	3,5565	0,3776	.0,0905	7,93e-4	0,1	628	1859,51	0,6	102,12	1,49	308,40	213,41

Component	K_1	K_2	$-K_3$	$A[m^2]$	A_{min}	A_{max}	C_p^0	n	C_p^1	B_1	B_2	$C_{BEC}2001$	$C_{BEC}2017$
EVA	4,1884	-0,250	0,1974	0,017	10	1000	13661,5	0,6	305,80	0,96	1,2	663,57	460,70
HX1	4,1884	-0,250	0,1974	8,9e-2	10	1000	13661,5	0,6	202,56	0,96	1,2	305.175	305,17
HX2	4,1884	-0,250	0,1974	0,0105	10	1000	13661,5	0,6	223,71	0,96	1,2	485.44	337.03

Component	C_{BEC} *2017*	*EPCC*	*TPC*	*TOC*	*TASC*
AFB	144,39	155,94	202,72	243,67	271,45
STR	213,41	230,48	299,62	360,15	401,21
EVA	460,70	497,56	646,82	777,48	866,11
HX1	305,17	329,58	428,46	515,00	573,71
HX2	337.03	364,00	473,20	568,78	633,61

Adding at plant cost the cost of a SAFCell (2584 euros) we arrive at the total cost of 7603 euros.

CONCLUSIONS

The aim of this work is to compare a known technology (SOFC) with an emerging technology (SAFCell). This new type of cell was hypothesized at the beginning of the 2000s, exploiting the studies of various experts on a new type of materials: solid acids. These particular elements have the characteristic of increasing their conductivity by two orders of magnitude when they reach the temperature of 200 ° C. In the study a SAFCell cell fed with methanol was taken into account to meet the energy needs of a mountain cabin. In this way you can avoid connecting the house to the methane distribution network, reducing transport costs in case of particularly isolated places. Taking real consumption data, various simulations were carried out in order to guarantee the adequate electrical energy required by the various domestic loads. Choosing two representative days of winter and summer consumption, a nominal power of 1500 W was set, making the cell work continuously for 24 hours. We then went on to investigate the actual costs that one technology has compared to another. From the point of view of fuel consumption, it has been seen that despite the cost of methane is lower than that of methanol, the flow rate in a SAFCell plant is much lower, allowing a saving of about 0.75 euros per day. As for the plant itself, it has been seen that the installation of a SOFC requires components in addition to an SAFCell: two compressors and two heat exchangers. There is therefore considerable savings from the point of view of plant engineering due to a much simpler system. Furthermore, there are substantial differences between the costs of the individual cells. While in fact a SOFC reaching temperatures of about 800 ° C requires high-quality (ceramic) construction materials, a SAFCell with lower operating temperatures can be constructed using cheaper materials. The savings are therefore in the order of 9,000 euros, a respectable expense. There are therefore several advantages, both economic and energy. In addition, the thermal recovery of the cell is not indifferent, thus being able to use the SAFCell also in a cogeneration system. Last but not least, the use of a liquid fuel allows to reduce the risks in the phase of both storage and actual use of the fuel. For all these reasons the SAFCell have all the necessary requirements to become the cells of the future, above all for those environments that signify to be independent from an energy point of view.

Bibliography

[1] https://ec.europa.eu/clima/change/causes_it. (s.d.).

[2] Solid acid proton conductors: from laboratory curiosities to fuel cell electrolytes Sossina M. Haile,* Calum R. I. Chisholm,w Kenji Sasaki, Dane A. Boysenw and Tetsuya Udaz

[3] High-Performance Solid Acid Fuel Cells Through Humidity Stabilization Dane A. Boysen, Tetsuya Uda, Calum R. I. Chisholm, Sossina M. Haile*

[4] Intermediate temperature fuel cells with electrolytes based on oxyacid salts
Bin Zhu, Bengt-Erik Mellander Department of Physics, Chalmers University of Technology, 412 96 Goth

[5] Electrochemical Characterization of Solid Acid Fuel Cell Electrodes.,Kenji Alexander Sasaki

[6] Materials for fuel-cell technologies, Brian C. H. Steele* & Angelika Heinzel†‡

[7] SAFC Overview & Opportunities-public – Chisholm

[8] Solid acid proton conductors: from laboratory curiosities to fuel cell electrolytes Sossina M. Haile,* Calum R. I. Chisholm,w Kenji Sasaki, Dane A. Boysenw and Tetsuya Udaz

[9] Effect of water vapor on proton conduction of cesium dihydrogen phosphateand application to intermediate temperature fuel cells, Junichiro Otomo, Takanori Tamaki, Satoru Nishida, Shuqiang Wang, Masaru Ogura

[10] Boysen, D.A. and Haile, S.M., *Chem. Mater.*, 2003, vol. 15, p. 727.

[11] Y.Taninouchietal. SolidStateIonics178,1648-1653(2008)

[12] T.UdaandS. M.Haile, Electrochem.SolidStateLett.8, A245-A246(2005)

[13] Solidacidsasfuelcellelectrolytes, Sossina M. Haile, Dane A. Boysen, Calum R. I. Chisholm & Ryan B. Merle

[14] An Oxide Ion and Proton Co-Ion Conducting Sn0.9In0.1P2O7 Electrolyte for IntermediateTemperature Fuel Cells , Xilin Chen, Chunsheng Wang

[15] https://www.eni.com/docs/it_IT/eni-com/media/eventi/docs-accordo-fca/Metanolo-scheda.pdf

[16] Beyond Oil and Gas: The Methanol Economy**,** George A. Olah, Alain Goeppert, G. K. Surya

[17] A.L. Dicks, Hydrogen generation from natural gas for the fuel cell systems of tomorrow, J. Power Sources 61 (1996) 113–124

[18] K. Ledjeff-Hey, V. Formanski, T. Kalk, J. Roes, Compact hydrogen production systems for solid polymer fuel cells, J. Power Sources 71 (1998) 199–207

[19] M. Zanfir, A. Gavriilidis, Catalytic combustion assisted methane steam reforming in a catalytic plate reactor, Chem. Eng. Sci. 58 (2003) 3947–3960.

[20] Development of a 1.2 kW Solid Acid Fuel Cell Stack for Diesel APUs FC Seminar, Nordic Power Systems AS, Dag Overbo, Calum Chisholm

[21] https://luce-gas.it/trasloco/allacciamento

[22] www.enerecosrl.com/public/files/pubbedole.pdf

[23] https://enigaseluce.com/offerta/casa/gas-e-luce

[24] http://www.energeticambiente.it/biodiesel-fai-da-te/14741483-prezzo-metanolo.html

[25] https://www.tesla.com/it_IT/powerwall?redirect=no

[26] Analysis, Synthesis and Design of Chemical Processes, R. Turton, R. Bailie

[27] NETL, Cost estimation methodology for NETL assessments of power plant performance,2001